

Entwined Dimers Formation from Self-Complementary bis-Acridiniums

H.-P. Jacquot de Rouville,^{*a,b} Nathalie Zorn,^c Emmanuelle Leize-Wagner,^c V. Heitz^{*a}

^aUniv Paris Diderot, Sorbonne Paris Cite, ITODYS, UMR CNRS 7086, 15 rue J-A de Baif, 75013 Paris, France

E-mail : h-p.jacquot@univ-paris-diderot.fr

^bLaboratoire de Synthèse des Assemblages Moléculaires Multifonctionnels, Institut de Chimie de Strasbourg, CNRS/UMR 7177, 4, rue Blaise Pascal, 67000 Strasbourg, France

E-mail : v.heitz@unistra.fr

E-mail : hpjacquot@unistra.fr

^cLaboratoire de Spectrométrie de Masse des Interactions et des Systèmes (LSMIS), UMR 7140 (Unistra-CNRS), Université de Strasbourg, France

Supporting Information

Table of Contents

1. Material and Methods.....	S1
2. Synthesis.....	S2
3 Structural Characterizations of the Synthesized Compounds.....	S6
Characterizations of 2·PF₆ (¹H, ¹³C NMR and ESI-MS).....	S6
Characterizations of 3 (¹H, ¹³C NMR and ESI-MS).....	S8
Characterizations of 4 (¹H, ¹³C NMR and ESI-MS).....	S10
Characterizations of 5 (¹H, ¹³C NMR and ESI-MS).....	S12
Characterizations of the equilibrium between 1²⁺ and (□)₂⁺.....	S14
Characterizations of the ion pair in (1)₂·4PF₆.....	S29
4 UV-Vis Characterization of 1·2PF₆.....	S31
5. Crystallographic Data of (1)₂·4PF₆.....	S32
6. References.....	S33

1. Material and General Methods.

Synthesis. All chemicals were of the best commercially available grade and used without further purification. 10-Methyl-9(10H)-acridone was synthesized according to previously reported procedure.^[S1] All compounds were synthesized using schlenk techniques and were fully characterized by 1D (¹H, ¹³C{¹H}, ³¹P{¹H} and ¹⁹F{¹H}) and 2D (COSY, HSQC and HMBC) NMR experiments and by mass spectrometry experiments. THF was dried using drystation GT S100 or distilled over sodium/benzophenone before use. Anhydrous DMF was purchased from ACROS organics. Column chromatography was carried out using silica gel (Merck, silica gel 60, 63–200 or 40–63 μ m). Mass spectra were obtained by using a Bruker MicroTOF spectrometer in electrospray mode (ESI). Nuclear magnetic resonance (NMR) spectra for ¹H were acquired on Bruker AVANCE 300, 400, 500 and 600 spectrometers. ¹³C spectra were acquired on a Bruker AVANCE 500 spectrometer. ¹⁹F spectra were acquired on a Bruker AVANCE 300 spectrometer. The ¹H and ¹³C spectra were referenced to residual solvent peaks^[S2]. Measures of self-diffusion coefficients were performed on a Bruker 600 MHz spectrometer-Avance III, equipped with a BBI probe (Bruker BBI probe, developing a pulse field gradient of 5 G/cm/A). The sample was thermostated at 298 K unless otherwise stipulated. Diffusion NMR data were acquired using a Stimulated Echo pulse sequence with bipolar z gradients. Limited Eddy current delay was fixed to 5 ms. The diffusion time and the duration of the gradients were optimized for each sample. A recycling delay of at least 5 s was respected between scans. DOSY spectra were generated by the DOSY module of the software Topspin to build the diffusion dimension. The diffusion coefficients were compared to CH₃CN or H₂O as an internal standards ($\eta(\text{CD}_3\text{CN}) = 3.57 \times 10^{-4}$ Pa.s and $\eta(\text{D}_2\text{O}) = 1.13 \times 10^{-3}$ Pa.s). UV–visible spectra were recorded on a Kontron Instruments UVIKON 860 spectrometer at 21 °C with a 1 cm path cell. The hydrodynamic radius (R_H) was calculated from the Stokes-Einstein equation assuming a spherical model^[S3] and using pre-determined solvent viscosity values.^[S4]

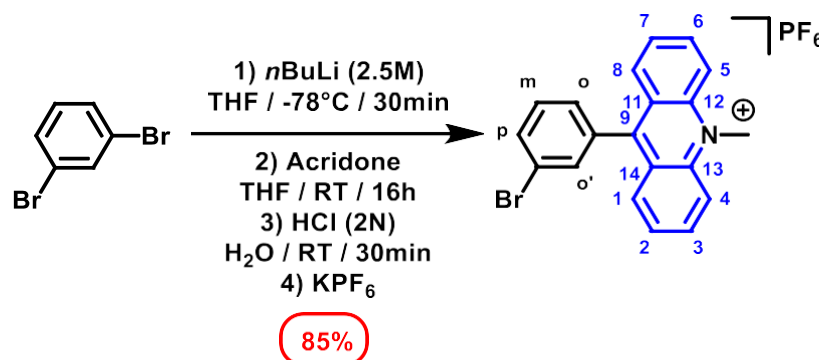
Crystallographic Method.

The crystals were placed in oil, and a single crystal was selected, mounted on a glass fibre and placed in a low-temperature N₂ stream. X-ray diffraction data collection was carried out on a Bruker APEX II DUO Kappa-CCD diffractometer equipped with an Oxford Cryosystem liquid N₂ device, using Mo-K α radiation ($\lambda = 0.71073$ Å). The crystal-detector distance was 38mm. The cell parameters were determined (APEX2 software)^[S5] from reflections taken from three sets of 6 frames, each at 10s exposure. The structure was solved using the program SHELXT-2014.^[S6] The refinement and all further calculations were carried out using SHELXL-2014.^[S7] The H-atoms were included in calculated positions and treated as riding atoms using SHELXL default parameters. The non-H atoms were refined anisotropically, using weighted full-matrix least-squares on F². A semi-empirical absorption correction was applied using SADABS in APEX2^[S5]; transmission factors: Tmin/Tmax = 0.6655/0.7456.

The fluorine atoms F1, F3, F5, F6, F8, F10, F11, F12, F14, F16, F17, F18, F19, F20, F21, F22, F23 and F24 from the counter-anions are disordered over two positions.

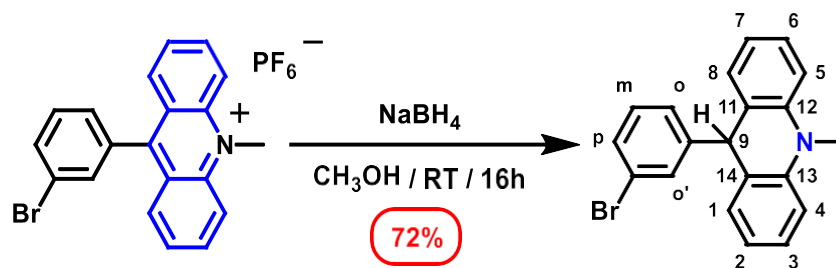
2. Synthesis

9-(3-Bromophenyl)-10-methylacridin-10-ium (2·PF₆)



To a solution of 1,3-dibromobenzene (580 μ L, 4.78 mmol, 1 eq) in dry THF (20 mL), was added a 2.5M solution of *n*BuLi (1.91 mL, 4.78 mmol, 1 eq) in hexanes at -78°C . After 20 minutes at -78°C , 10-methyl-9(10H)-acridone^[S1] (1.00 g, 4.78 mmol, 1 eq) was added dropwise. The mixture was further stirred at -78°C for 2 hours, and allowed to room temperature overnight. After addition of a concentrated solution of HCl (37 wt. %) in H₂O (30 mL), the reaction mixture was stirred at RT for 30 min. The solution was poured into an aqueous solution of KPF₆ (6 g in 150 mL). After filtration, the crude product was washed with H₂O (3 x 30 mL). When necessary, the compound was recrystallized from CH₃CN by addition of Et₂O. The desired product was obtained as a yellowish solid in 85% yield (2.01 g). ¹H NMR (400 MHz, CD₃CN, 298 K): δ (ppm) = 8.64 (d, *J* = 9.0 Hz, 2H, H_{4/5}), 8.40 (ddd, *J* = 9.0, 7.0, 1.5 Hz, 2H, H_{3/6}), 8.02 (dd, *J* = 9.0, 1.5 Hz, 2H, H_{1/8}), 7.94 (ddd, *J* = 8.0, 2.0, 1.0 Hz, 1H, H_p), 7.86 (ddd, *J* = 9.0, 7.0, 1.5 Hz, 2H, H_{2/7}), 7.72 (t, *J* = 2.0 Hz, 1H, H_{o'}), 7.67 (t, *J* = 8.0 Hz, 1H, H_m), 7.52 (ddd, *J* = 8.0, 2.0, 1.0 Hz, 1H, H_p), 4.87 (s, 3H, N-Me). ¹³C{¹H} NMR (100 MHz, CD₃CN, 298 K): δ (ppm) = 160.4 (s, C₉), 142.7 (s, C_{11/14}), 139.8 (s, C_{3/6}), 136.4 (s, C_{q-Ph}), 134.2 (s, C_p), 133.3 (s, C_{o'}), 131.8 (s, C_m), 130.9 (s, C_{1/8}), 129.9 (s, C_p), 129.0 (s, C_{2/7}), 127.0 (s, C_{12/13}), 123.6 (s, C_{C-Br}), 119.5 (s, C_{4/5}), 39.8 (s, N-Me). ¹⁹F{¹H} NMR (376 MHz, CD₃CN, 298 K): δ (ppm) = -72.8 (d, *J* = 706 Hz). ³¹P{¹H} NMR (162 MHz, CD₃CN, 298 K): δ (ppm) = -144.58 (hept, *J* = 706 Hz). MS (ESI-TOF): for C₂₀H₁₄BrN, *m/z*_{calc} = 348.04, *m/z*_{found} = 348.04 (100%, [M-PF₆]⁺).

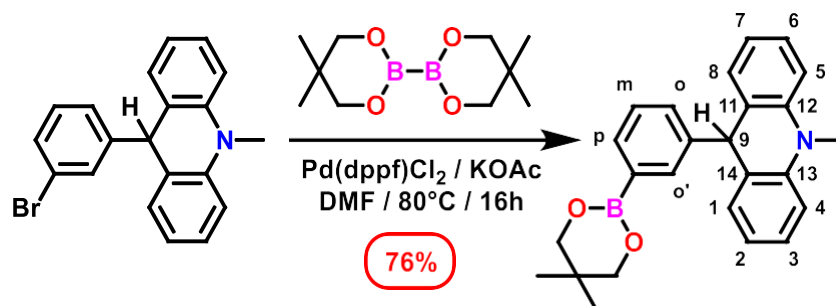
9-(3-Bromophenyl)-10-methyl-9,10-dihydroacridine (3)



To a solution of 9-(3-bromophenyl)-10-methylacridin-10-ium (206 mg, 0.49 mmol, 1 eq) in dry CH₃OH (20 mL), was added portion wise NaBH₄ (187 mg, 4.96 mmol, 10 eq) at 0°C. The reaction

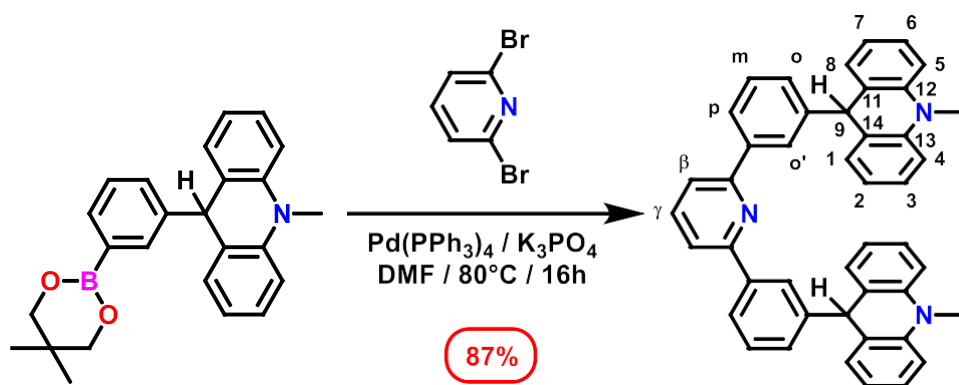
mixture was heated at RT for 16h. After evaporation of solvents, the crude product was purified by column chromatography (SiO₂, CH₂Cl₂). The desired product was obtained as a colorless solid in 72% yield (125 mg). ¹H NMR (400 MHz, CDCl₃, 298 K): δ (ppm) = 7.21 – 7.12 (m, 4H, H_{3/6-o-p}), 7.10 (dd, J = 7.5, 1.5 Hz, 2H, H_{1/8}), 6.97 (t, J = 7.5 Hz, 1H, H_m), 6.93 (dt, J = 7.5, 1.5 Hz, 1H, H_{o'}), 6.90 – 6.85 (m, 4H, H_{2/7-4/5}), 5.07 (s, 1H, H₉), 3.33 (s, 3H, N-Me). ¹³C{¹H} NMR (100 MHz, CDCl₃, 298 K): δ (ppm) = 147.3 (s, C_{q-Ph}), 142.3 (s, C_{12/13}), 130.5 (s, C_{11/14}), 130.0 (s, C_m), 129.4 (s), 128.6 (s, C_{1/8}), 127.5 (s, C_{3/6}), 126.1 (s), 126.0 (s), 122.5 (s), 120.8 (s, C_{2/7}), 112.5 (s, C_{4/5}), 48.3 (s, C₉), 33.1 (s, N-Me). MS (ESI-TOF): for C₂₀H₁₇BrN, m/z_{calc} = 350.05, m/z_{found} = 350.05 (100%, [M+H]⁺).

9-(3-(5,5-Dimethyl-1,3,2-dioxaborinan-2-yl)phenyl)-10-methyl-9,10-dihydroacridine (4)

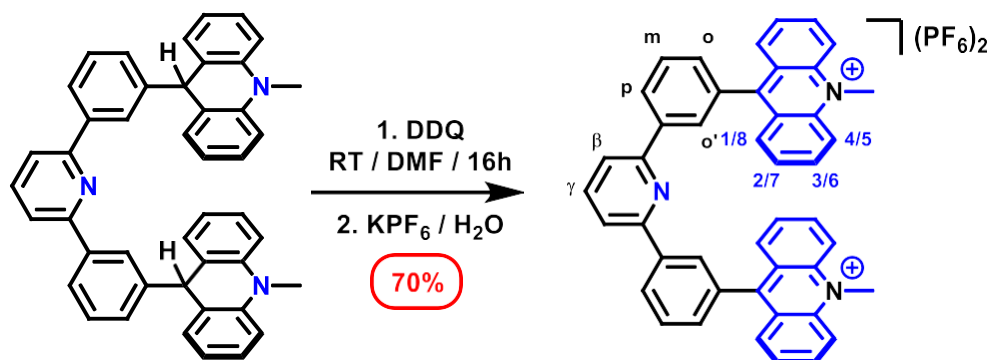


To a solution of 9-(3-bromophenyl)-10-methyl-9,10-dihydroacridine (477 mg, 1.36 mmol, 1eq.) and bis(neopentyl glycolato)diboron (338 mg, 1.50 mmol, 1.1 eq.) in dry and degassed DMF (40 mL), were added Pd(dppf)Cl₂ (76 mg, 0.13 mmol, 10%) and KOAc (400 mg, 4.08 mmol, 3 eq.). The reaction mixture was heated at 80°C for 16h. After evaporation of solvents, the crude product was purified by column chromatography (SiO₂, cyclohexane / CH₂Cl₂ – 7:3). The desired product was obtained as a colorless solid in 76% yield (399 mg). ¹H NMR (400 MHz, CDCl₃, 298 K): δ (ppm) = 7.75 (s, 1H, H_{o'}), 7.59 (dt, J = 7.0, 1.5 Hz, 1H, H_o), 7.24 – 7.16 (m, 3H, H_{3/6-p}), 7.13 (dd, J = 8.0, 2H, H_{1/8}), 7.08 (dt, J = 1.5 Hz, 1H, H_m), 6.95 (d, J = 8.0 Hz, 2H, H_{4/5}), 6.89 (td, J = 7.4, 1.1 Hz, 2H, H_{2/7}), 5.21 (s, 1H, H₉), 3.74 (s, 4H, CH₂), 3.44 (s, 3H, N-Me), 1.34 (s, 6H, Me). ¹³C{¹H} NMR (100 MHz, CDCl₃, 298 K): δ (ppm) = 144.0 (s, C_{q-Ph}), 142.3 (s, C_{12/13}), 133.2 (s, C_{o'}), 132.0 (s, C_o), 130.3 (s, C_m), 128.6 (s, C_{1/8}), 127.9 (s, C_p), 127.2 (s, C_{3/6}), 127.1 (s, C_{11/14}), 120.6 (s, C_{2/7}), 112.2 (s, C_{4/5}), 72.2 (s, C_{CH2}), 48.6 (s, C₉), 33.1 (s, N-Me), 31.8 (s, C_q), 21.9 (s, Me). MS (ESI-TOF): for C₂₅H₂₅BNO₂, m/z_{calc} = 382.20, m/z_{found} = 382.20 (100%, [M-H]⁺).

Compound (5)



To a solution of 10-methyl-9-(3-(4,4,5,5-tetramethyl-1,3,2-dioxaborolan-2-yl)phenyl)-9,10-dihydroacridine (350 mg, 0.88 mmol, 2.1 eq.) and 2,6-dibromopyridine (100 mg, 0.42 mmol, 1 eq.) in degassed DMF (50 mL), was added $\text{Pd(PPh}_3)_4$ (48 mg, 0.09 mmol, 20%) and K_3PO_4 (267 mg, 1.26 mmol, 3 eq.). The reaction mixture was heated at 80°C for 16h. After evaporation of solvents, the crude product was purified by column chromatography (SiO_2 , cyclohexane / CH_2Cl_2 – 7:3). The desired product was obtained as a colorless solid in 87% yield (225 mg). ^1H NMR (400 MHz, CDCl_3 , 298 K): δ (ppm) = 7.93 (t, J = 2.0 Hz, 2H, $\text{H}_{\text{o'}}$), 7.88 (dt, J = 8.0, 2.0 Hz, 2H, H_{p}), 7.70 (t, J = 8.0 Hz, 1H, H_{γ}), 7.53 (d, J = 8.0 Hz, 2H, H_{β}), 7.34 (t, J = 8.0 Hz, 2H, H_{m}), 7.29 – 7.21 (m, 8H, $\text{H}_{1/8-3/6}$), 7.18 (d, J = 8.0 Hz, 2H, H_{o}), 7.01 – 6.90 (m, 8H, $\text{H}_{4/6-2/7}$), 3.43 (s, 6H, Me). $^{13}\text{C}\{^1\text{H}\}$ NMR (100 MHz, CDCl_3 , 298 K): δ (ppm) = 156.6 (s, C_{Py}), 145.0 (s, C_{Ph}), 142.5 (s, $\text{C}_{12/13}$), 139.4 (s, C_{Ph}), 137.2 (s, C_{γ}), 128.7 (s, C_{m}), 128.6 (s, $\text{C}_{3/6}$), 128.5 (s, $\text{C}_{\text{o'}}$), 127.3 (s, $\text{C}_{1/8}$), 126.8 (s, $\text{C}_{11/14}$), 126.4 (s, $\text{C}_{\text{q-Ph}}$), 125.0 (s, C_{p}), 120.7 (s, $\text{C}_{2/7}$), 118.3 (s, C_{β}), 112.3 (s, $\text{C}_{4/6}$), 48.5 (s, C_9), 33.1 (s, Me). HRMS (ESI-TOF): for $\text{C}_{45}\text{H}_{36}\text{N}_3$, $m/z_{\text{calc}} = 618.2904$, $m/z_{\text{found}} = 618.2911$ (100%, $[\text{M}+\text{H}]^+$).

Molecular Receptor 1·2PF₆

To a solution of **5** (140 mg, 0.226 mmol, 1 eq.) in DMF (15 mL), was added 2,3-dichloro-5,6-dicyano-1,4-benzoquinone (206 mg, 0.906 mmol, 4 eq.). The reaction mixture was stirred at room temperature for 16h. The mixture was poured into a saturated solution of KPF_6 (6 g) in H_2O (150 mL), affording a yellowish precipitate. The solution was filtered, washed with H_2O and ethanol. The desired product was obtained as a yellowish solid in 70% yield (143 mg). Characterization of $(\square)^{2+}$: ^1H NMR (600 MHz, CD_3CN , 238 K, $10^{-2} \text{ mol}\cdot\text{L}^{-1}$): δ (ppm) = 8.42 (d, J = 9.0 Hz, 4H,

$H_{4/5}$), 8.32 (s, 2H, H_{O^\bullet}), 8.17 (ddd, $J = 9.0, 6.5, 1.5$ Hz, 4H, $H_{3/6}$), 7.31 – 7.27 (m, 3H, $H_{2/7-\gamma}$), 7.08 – 7.04 (m, 6H, $H_{1/8-m}$), 6.94 (d, $J = 8.0$ Hz, 2H, H_o), 6.64 (d, $J = 8.0$ Hz, 2H, H_p), 6.47 (d, $J = 8.0$ Hz, 2H, H_β), 4.69 (s, 6H, N-Me). ^{13}C NMR (150 MHz, CD_3CN , 238 K, $10^{-2} \text{ mol}\cdot\text{L}^{-1}$): 159.8 (s, C_9), 152.5 (s, $C_{q-\text{Py}}$), 140.3, 138.9 (s, $C_{3/6}$), 136.3, 136.2 (s, C_γ), 133.2, 129.3 (s, C_m), 129.2 (s, C_o), 129.0 (s, $C_{1/8}$), 127.5 (s, $C_{2/7}$), 125.9 (s, C_p), 125.3 (s, C_{o^\bullet}), 125.2, 118.6 (s, $C_{4/5}$), 118.5 (s, C_β), 38.5 (s, Me). $^{19}\text{F}\{^1\text{H}\}$ NMR (564 MHz, CD_3CN , 298 K): δ (ppm) = -72.8 (d, $J = 706$ Hz). $^{31}\text{P}\{^1\text{H}\}$ NMR (242 MHz, CD_3CN , 298 K): δ (ppm) = -144.58 (hept, $J = 706$ Hz). ^1H NMR (500 MHz, D_2O , 298 K): δ (ppm) = 8.47 (d, $J = 9.3$ Hz, 4H, $H_{4/5}$), 8.40 (s, 2H, H_{O^\bullet}), 8.30 – 8.09 (m, 4H, $H_{3/6}$), 7.56 (t, $J = 8.0$ Hz, 1H, H_γ), 7.41 – 7.29 (m, 4H, $H_{2/7}$), 7.26-7.22 (m, 6H, $H_{1/8-m}$), 7.10 (d, $J = 7.0$ Hz, 2H, H_o), 6.89 (d, $J = 7.0$ Hz, 2H, H_p), 6.74 (d, $J = 8.0$ Hz, 2H, H_β), 4.79 (s, 6H, N-Me). $^{13}\text{C}\{^1\text{H}\}$ NMR (150 MHz, D_2O , 298 K): δ (ppm) = 160.1, 152.4, 140.3, 138.8 (s, $C_{3/6}$), 135.9 (s, C_γ), 135.8, 133.2, 129.7 (s, C_o), 129.0 (s, $C_{1/8}$), 128.9 (s, C_m), 127.0 (s, $C_{2/7}$), 126.4 (s, C_p), 125.2 (s, C_{o^\bullet}), 125.1, 118.4 (s, C_β), 118.0 (s, $C_{4/5}$), 37.8 (s, Me). HRMS (ESI-TOF): for $\text{C}_{45}\text{H}_{33}\text{N}_3$, $m/z_{\text{calc}} = 307.6332$, $m/z_{\text{found}} = 307.6362$ (100%, $[\text{M}]^{2+}$). UV/Vis (CH_3CN , 298 K): λ_{max} (nm) (ϵ ($\text{L}\cdot\text{mol}^{-1}\cdot\text{cm}^{-1}$)) = 307 (15300), 348 (15900), 361 (29850), 408 (10350), 425 (11900), 451 (7680). UV/Vis (H_2O , 298 K): λ_{max} (nm) (ϵ ($\text{L}\cdot\text{mol}^{-1}\cdot\text{cm}^{-1}$)) = 319 (7400), 325 (7400), 362 (14200), 409 (5300), 431 (5700), 457 (3700). Crystal data for **(1) \cdot 4PF₆**: $2(\text{C}_{45}\text{H}_{33}\text{N}_3)\cdot 4(\text{F}_6\text{P})\cdot \text{C}_2\text{H}_3\text{N}$, orange prism, crystal size 0.36 x 0.34 x 0.28 mm³, monoclinic, space group $P 2_1/c$, $a = 12.8107(4)$ Å, $b = 27.4670(10)$ Å, $c = 25.2827(10)$ Å, $\alpha = 90^\circ$, $\beta = 113.746(2)^\circ$, $\gamma = 90^\circ$, $V = 8143.1(5)$ Å³, $Z = 4$, $\rho_{\text{calc}} = 1.511$, $T = 173(2)$ K, $R_1(F^2 > 2\sigma F^2) = 0.0977$, $wR_2 = 0.2449$. Out of 87028 reflections a total of 19650 were unique. Crystallographic data (excluding structure factors) for the structures reported in this communication have been deposited with the Cambridge Crystallographic Data Center as supplementary publication no. CCDC-1856039

3. Structural Characterizations of the Synthesized Compounds

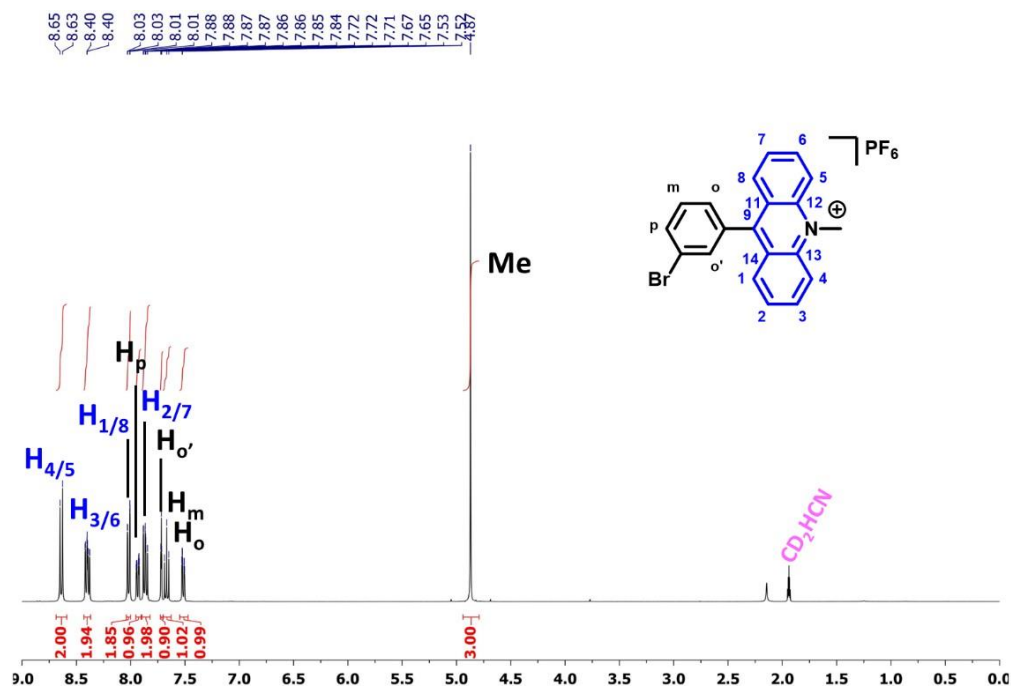


Figure S3.1: ^1H NMR (400 MHz, CD_3CN , 298 K) spectrum of **2**· PF_6 .

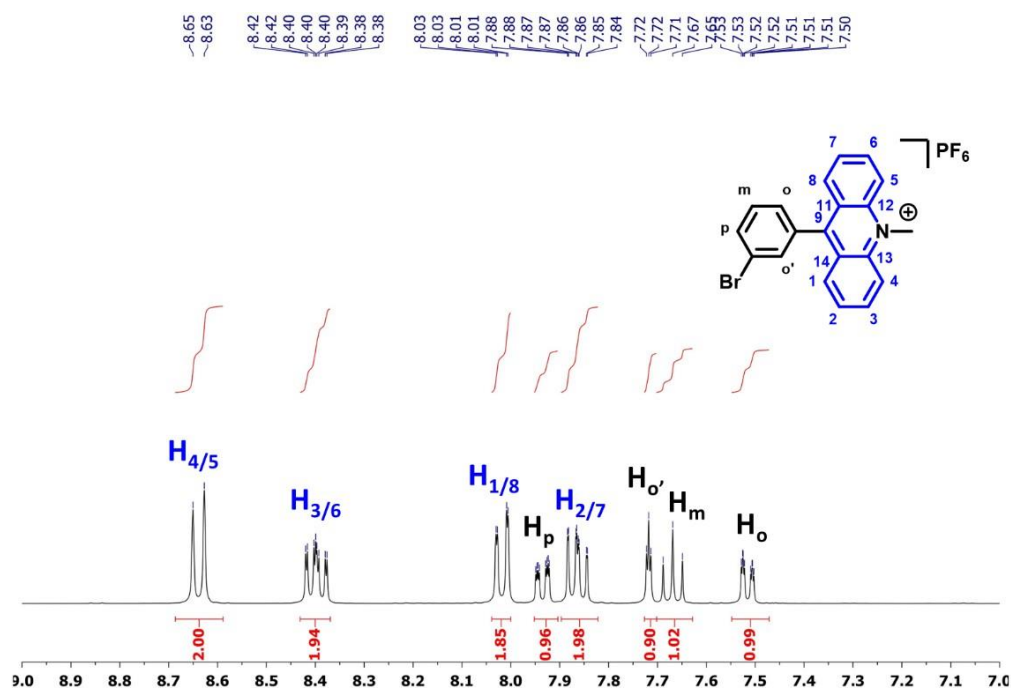


Figure S3.2: ^1H NMR (400 MHz, CD_3CN , 298 K) spectrum of **2**· PF_6 (zoom aromatic region).

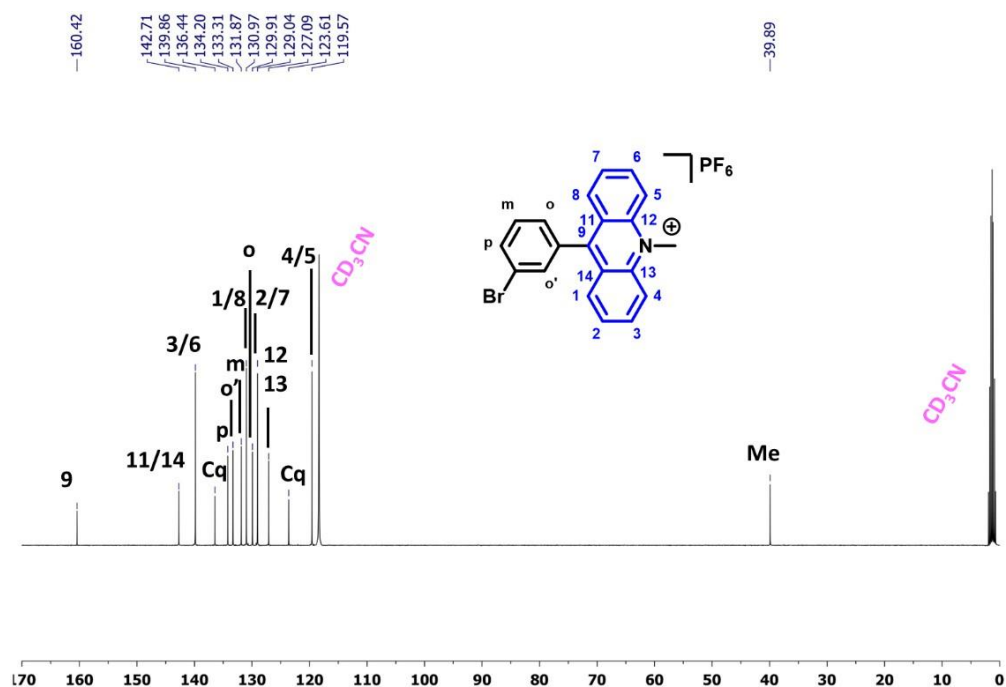


Figure S3.3: ¹³C NMR (100 MHz, CD₃CN, 298 K) spectrum of **2**·PF₆.

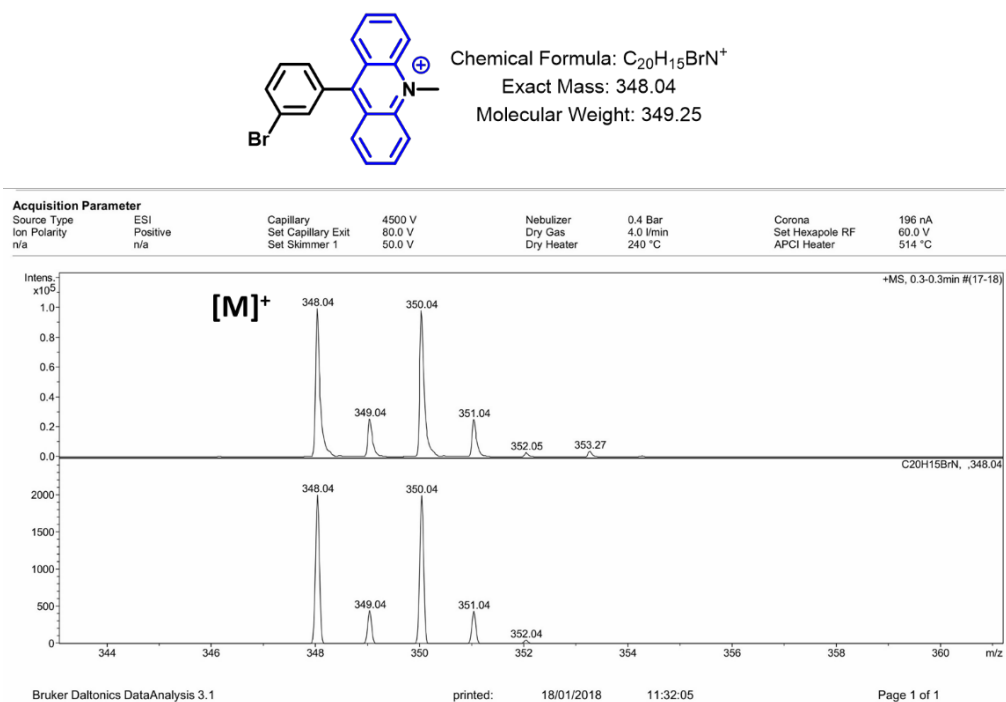


Figure S3.4: MS (ESI-TOF) of **2**·PF₆.

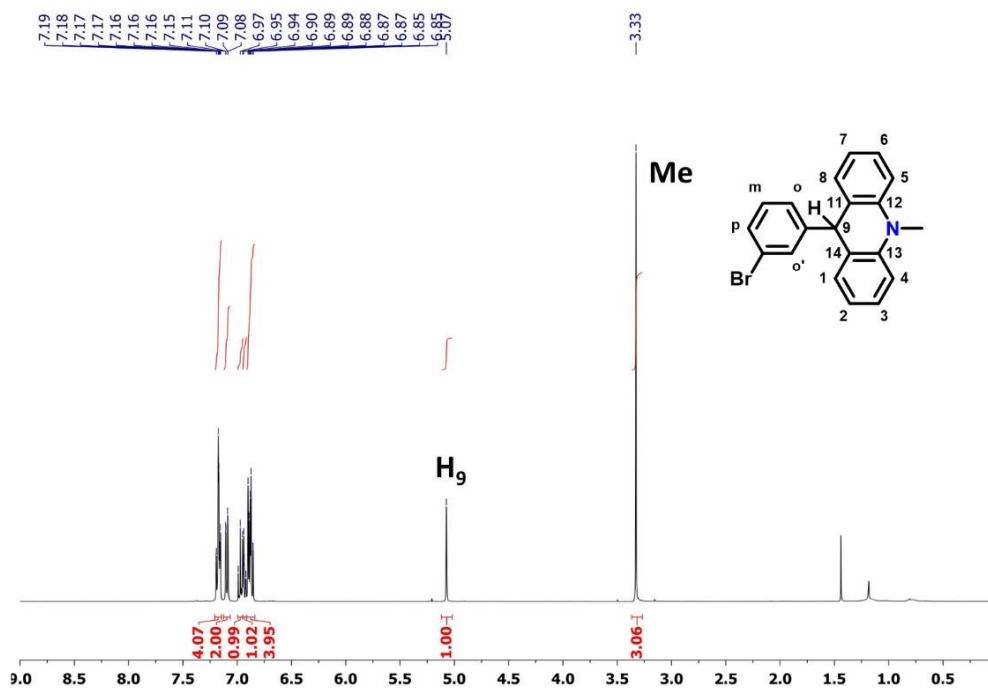


Figure S3.5: ¹H NMR (400 MHz, CDCl₃, 298 K) spectrum of **3**.

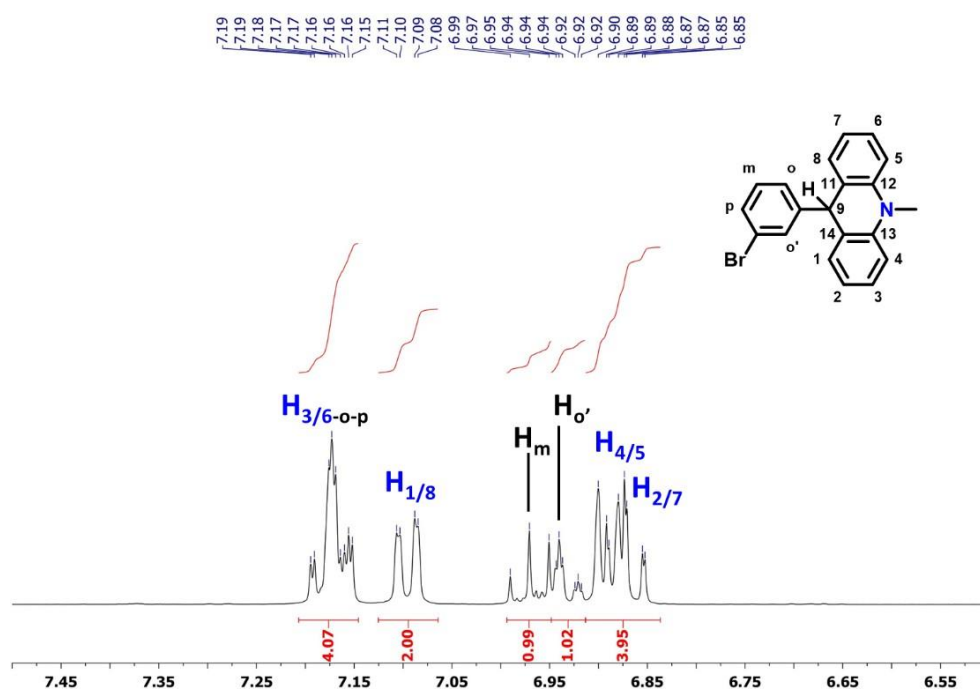


Figure S3.6: ¹H NMR (400 MHz, CDCl₃, 298 K) spectrum of **3** (zoom aromatic region).

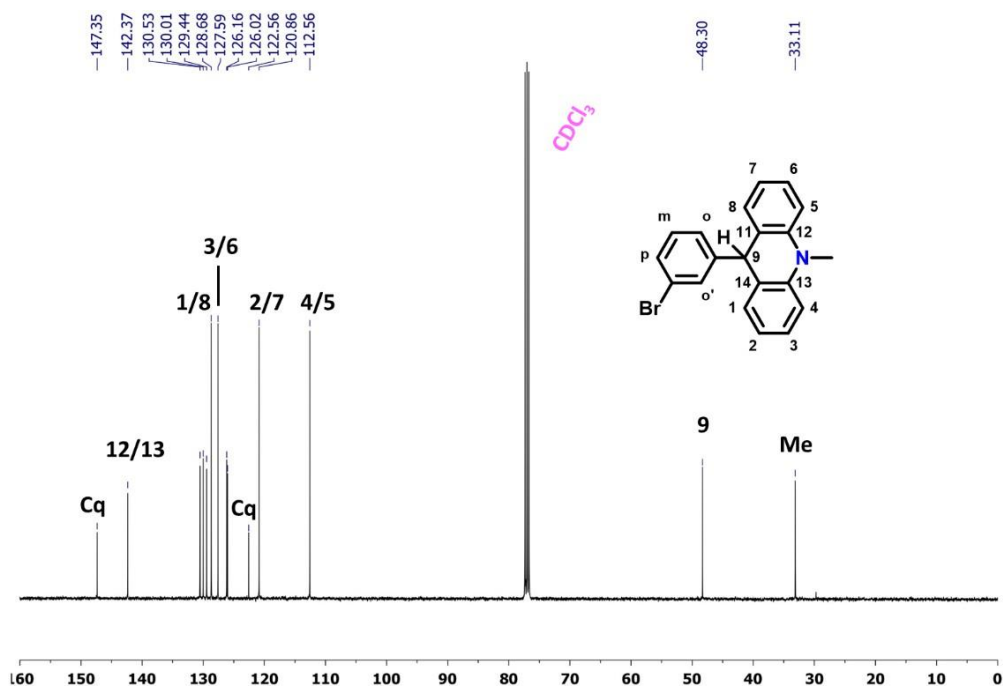


Figure S3.7: ^{13}C NMR (100 MHz, CDCl_3 , 298 K) spectrum of **3**.

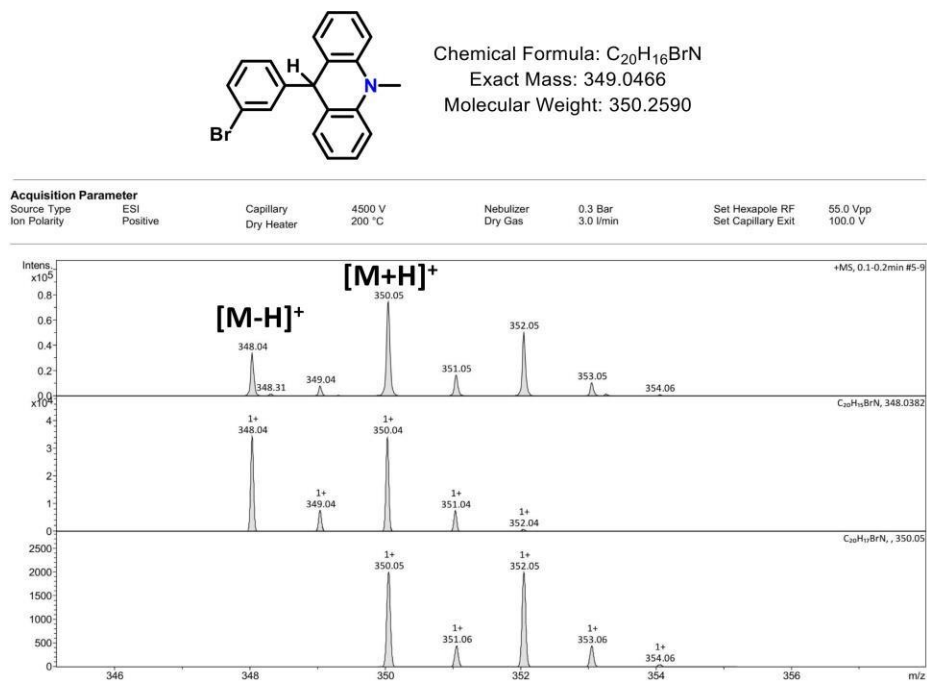
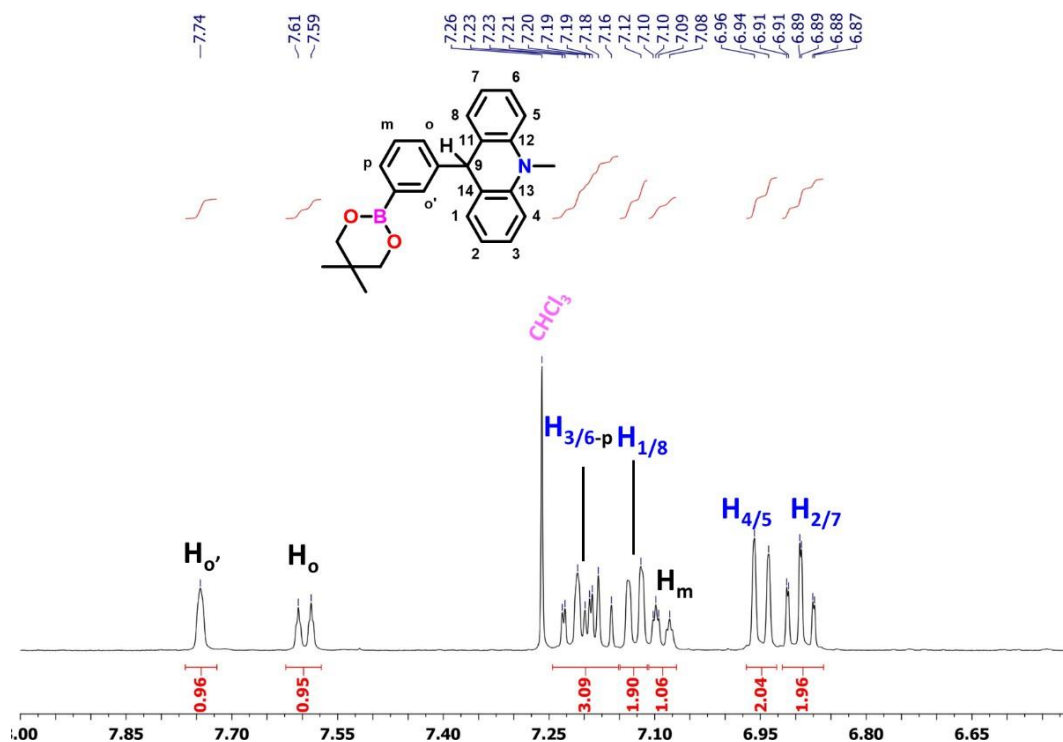
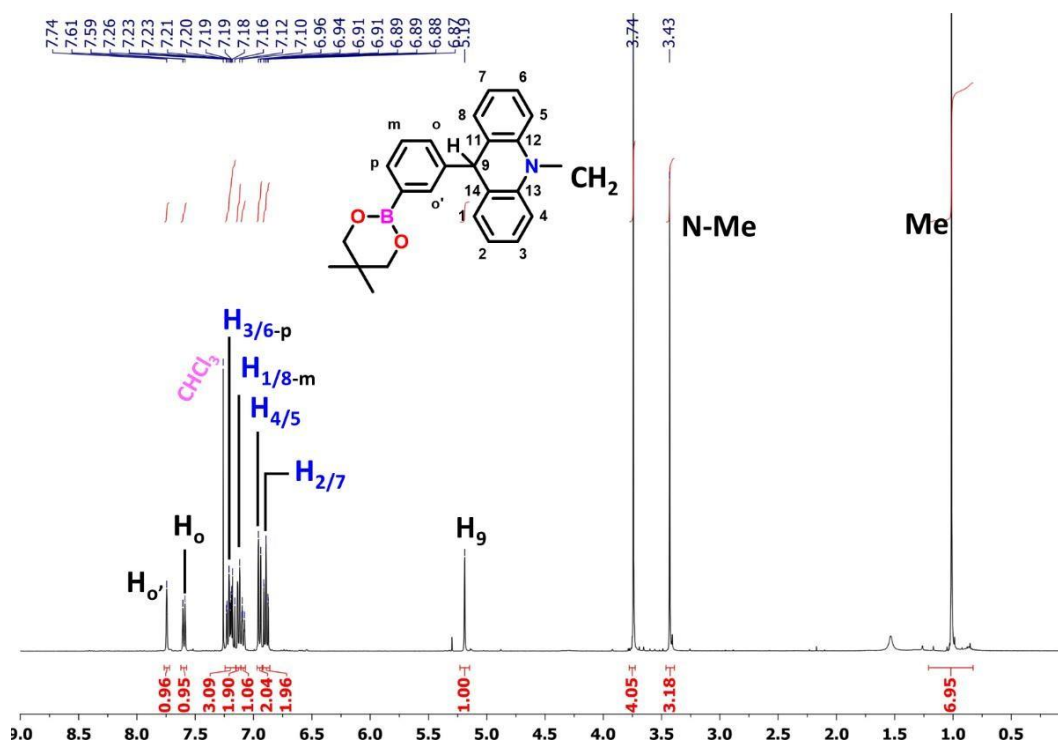


Figure S3.8: MS (ESI-TOF) of **3**.



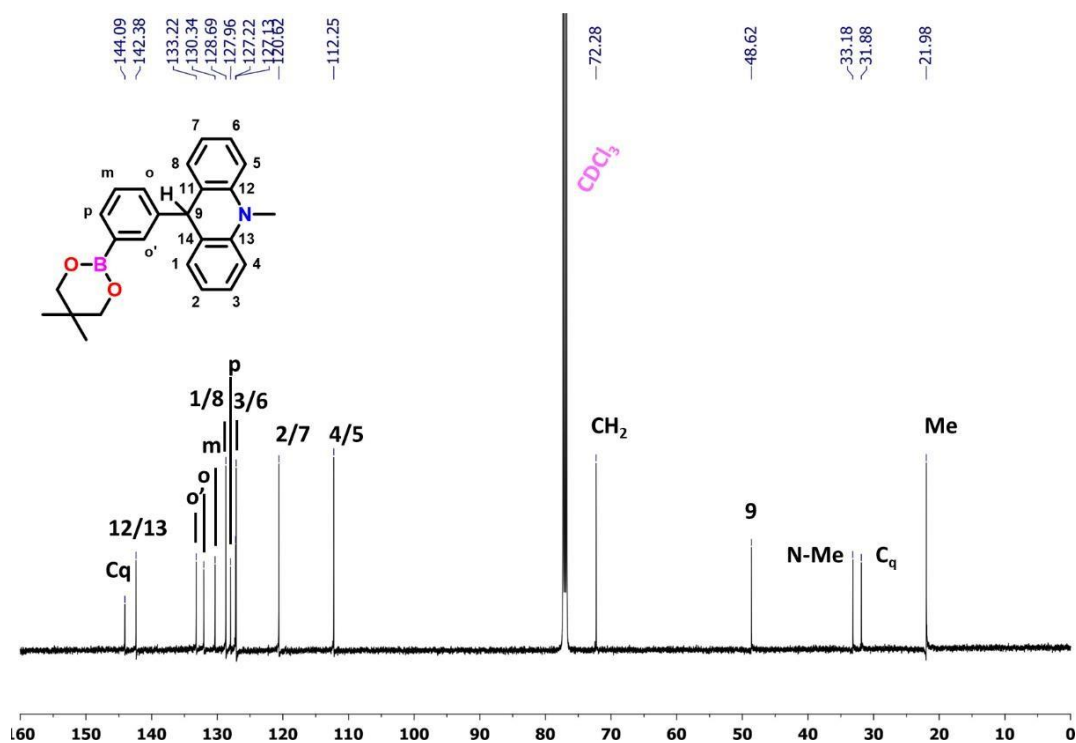


Figure S3.11: ^{13}C NMR (100 MHz, CDCl_3 , 298 K) spectrum of 4.

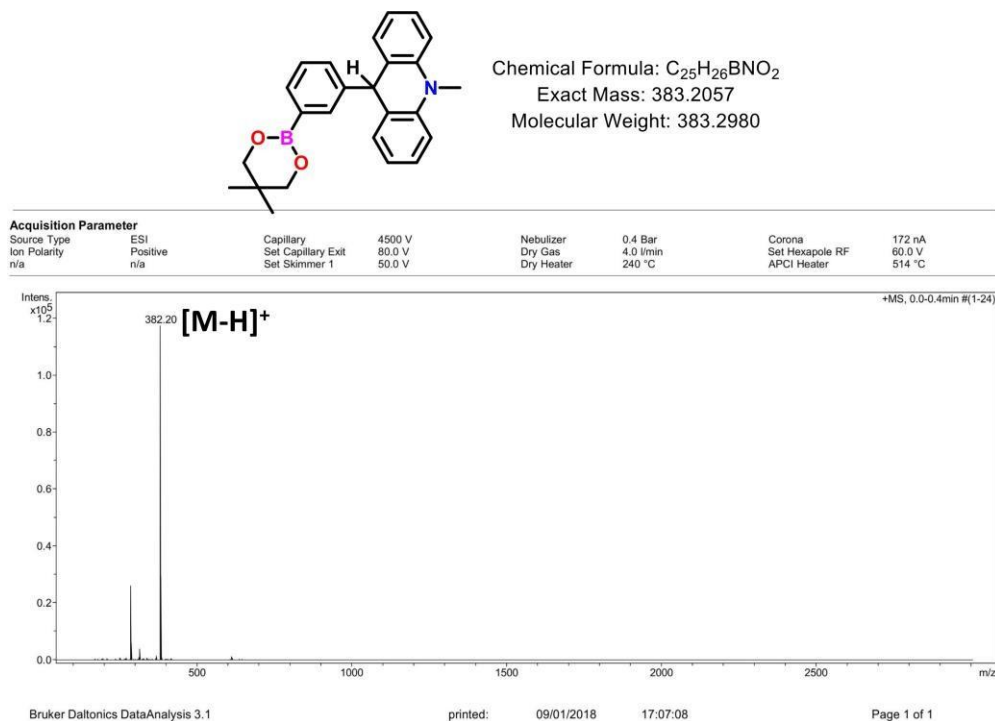


Figure S3.12: MS (ESI-TOF) of 4.

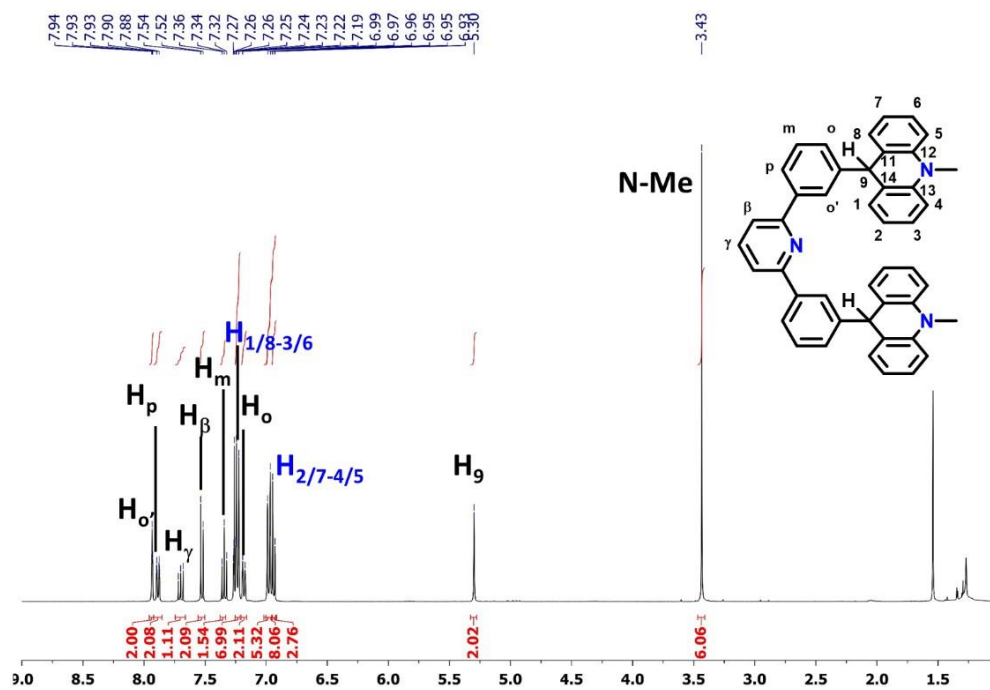


Figure S3.13: ^1H NMR (400 MHz, CDCl_3 , 298 K) spectrum of **5**.

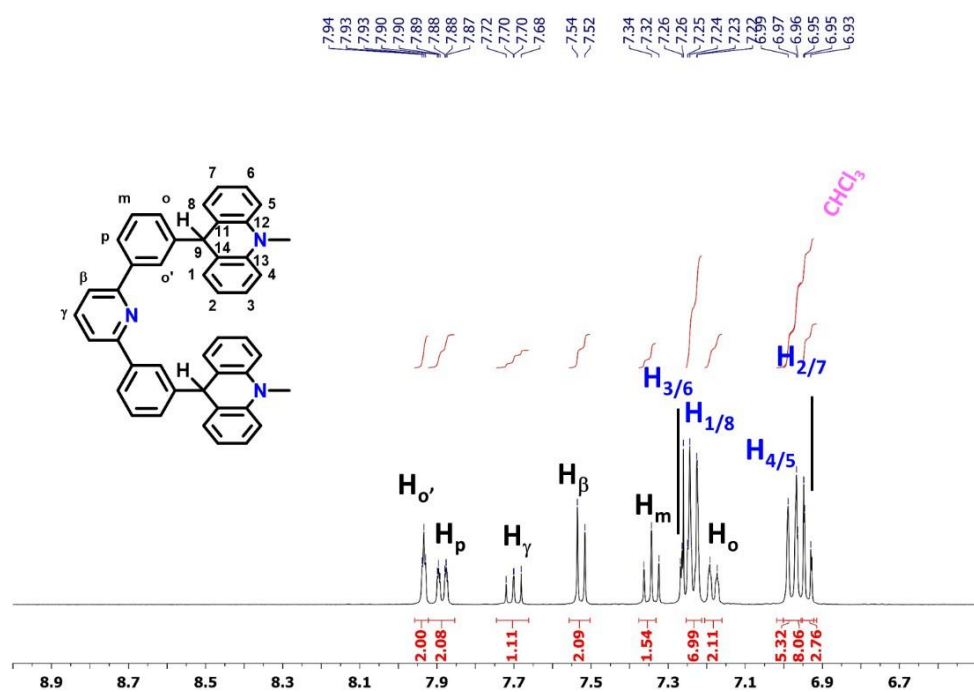


Figure S3.14: ^1H NMR (400 MHz, CDCl_3 , 298 K) spectrum of **5** (zoom aromatic region).

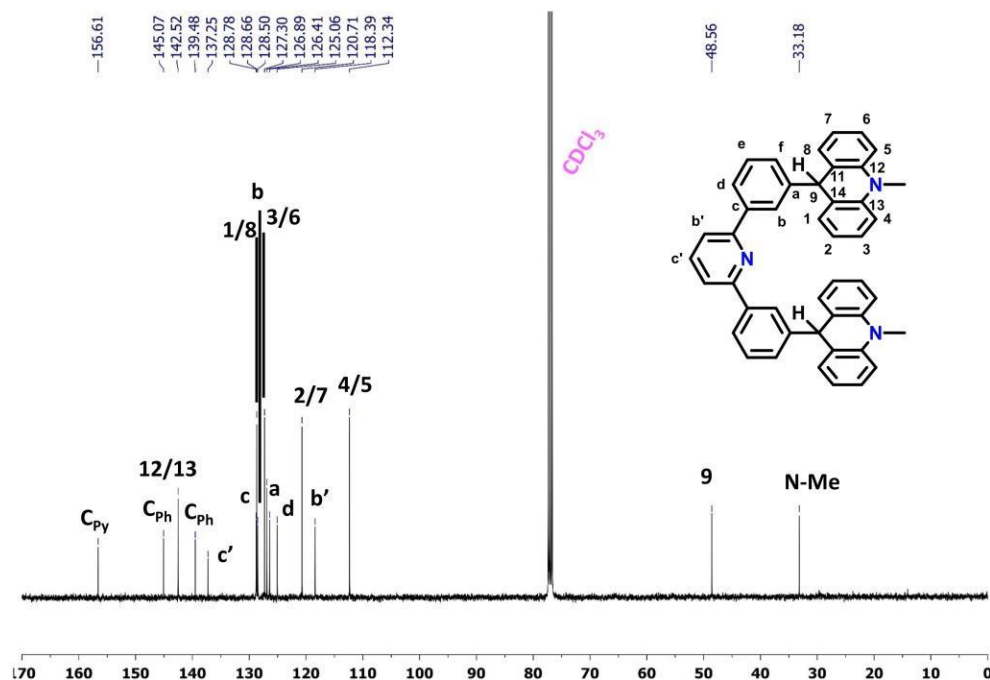


Figure S3.15: ^{13}C NMR (100 MHz, CDCl_3 , 298 K) spectrum of **5**.

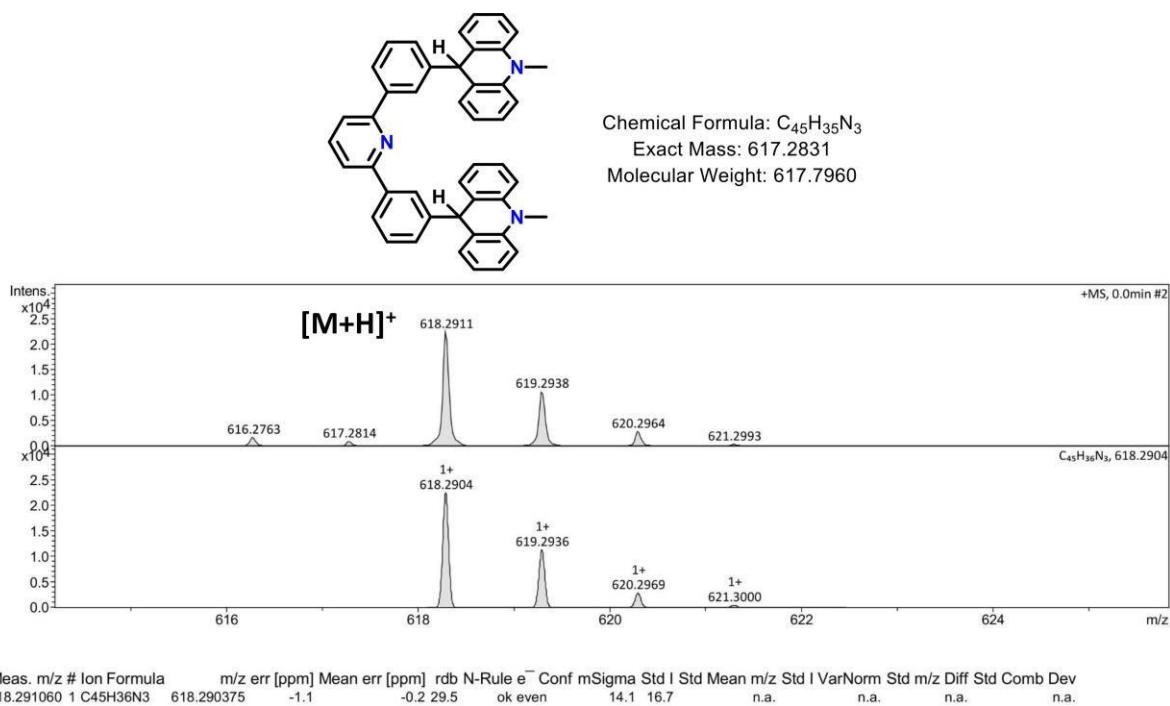


Figure S3.16: MS (ESI-TOF) of **5**.

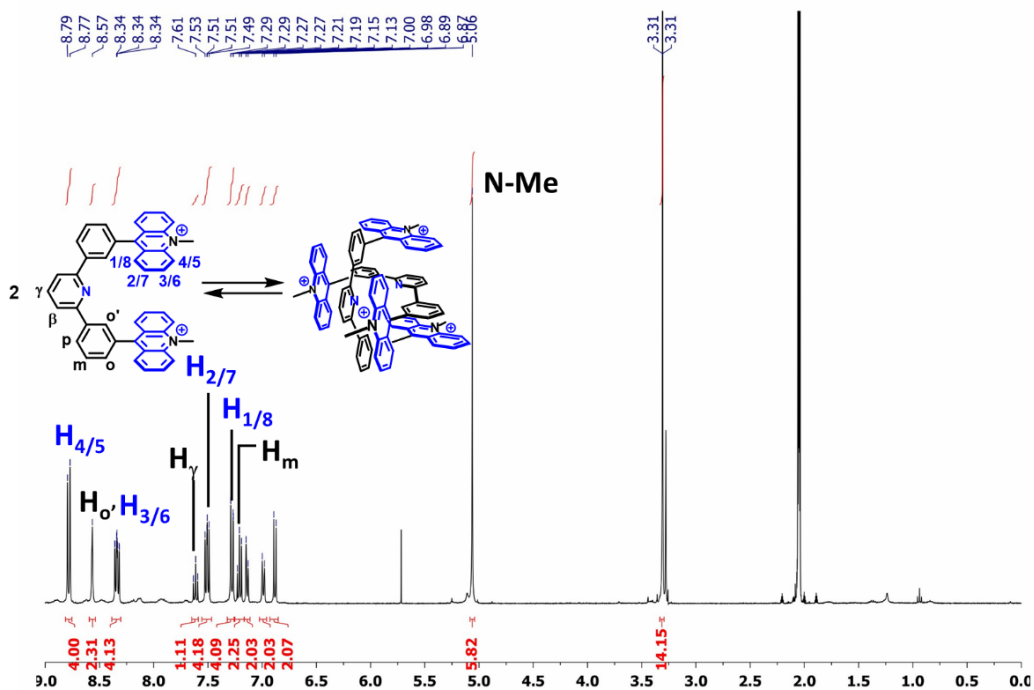


Figure S3.17: ^1H NMR (600 MHz, CD_3CN , 238 K) spectrum of the dimer of $(\mathbf{1})_2 \cdot 4\text{PF}_6$ ($c = 1 \cdot 10^{-2} \text{ mol} \cdot \text{L}^{-1}$).

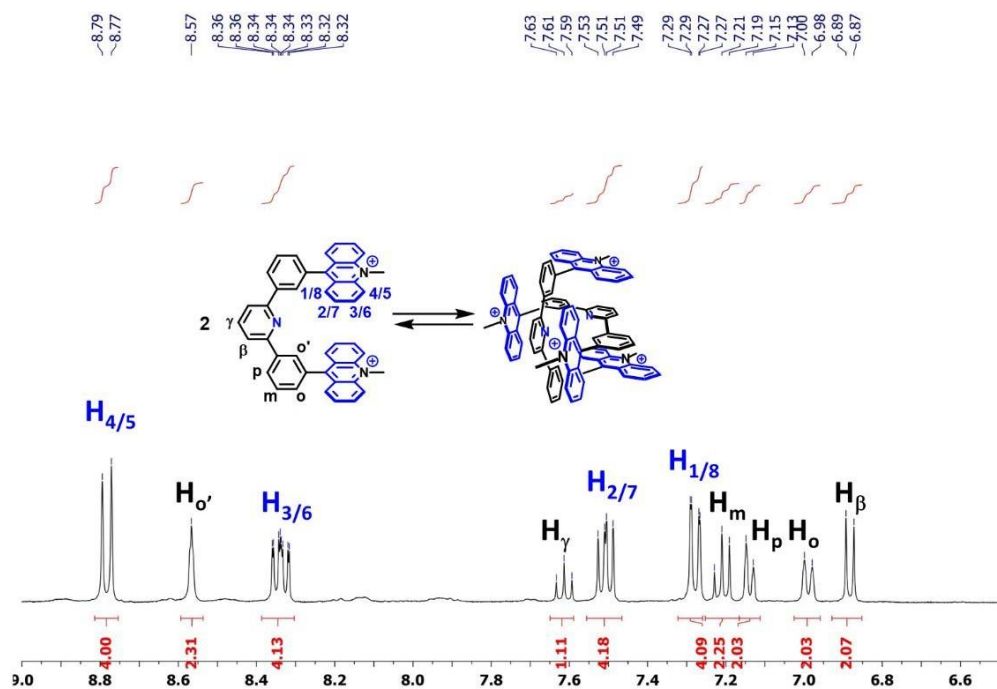


Figure S3.18: ^1H NMR (600 MHz, CD_3CN , 238 K) spectrum of the dimer of $(\mathbf{1})_2 \cdot 4\text{PF}_6$ ($c = 1 \cdot 10^{-2} \text{ mol} \cdot \text{L}^{-1}$; zoom aromatic region).

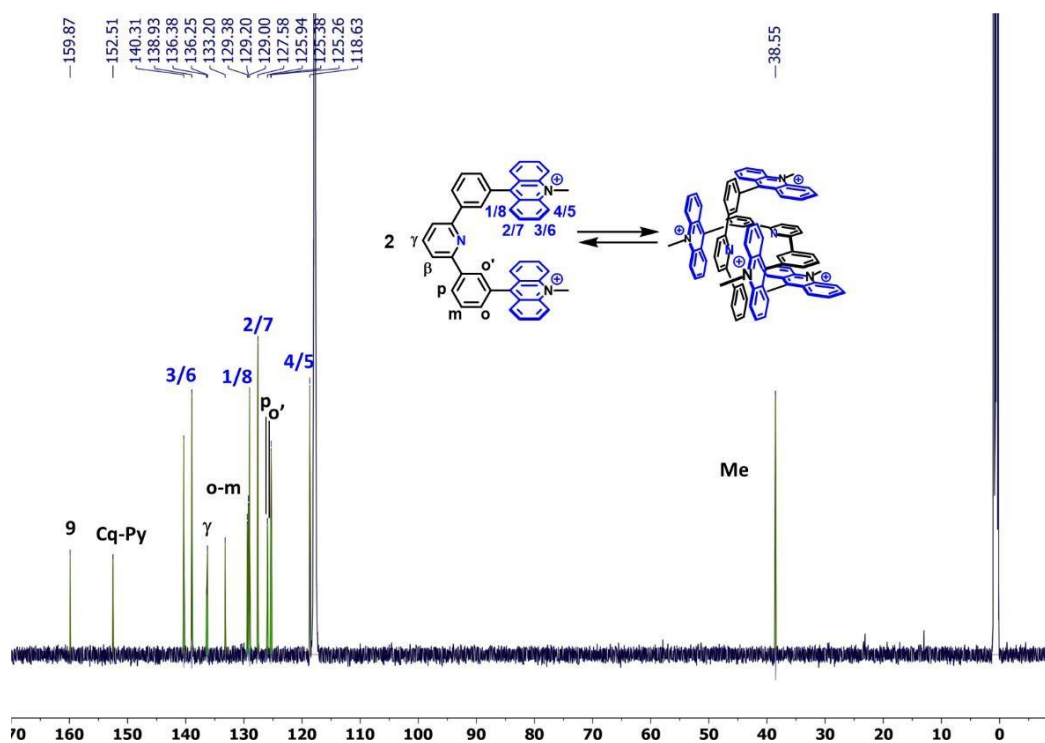


Figure S3.19: ^{13}C NMR (150 MHz, CD_3CN , 238 K) spectrum of the dimer of $(\mathbf{1})_2\cdot 4\text{PF}_6$ ($c = 1\cdot 10^{-2} \text{ mol}\cdot\text{L}^{-1}$).

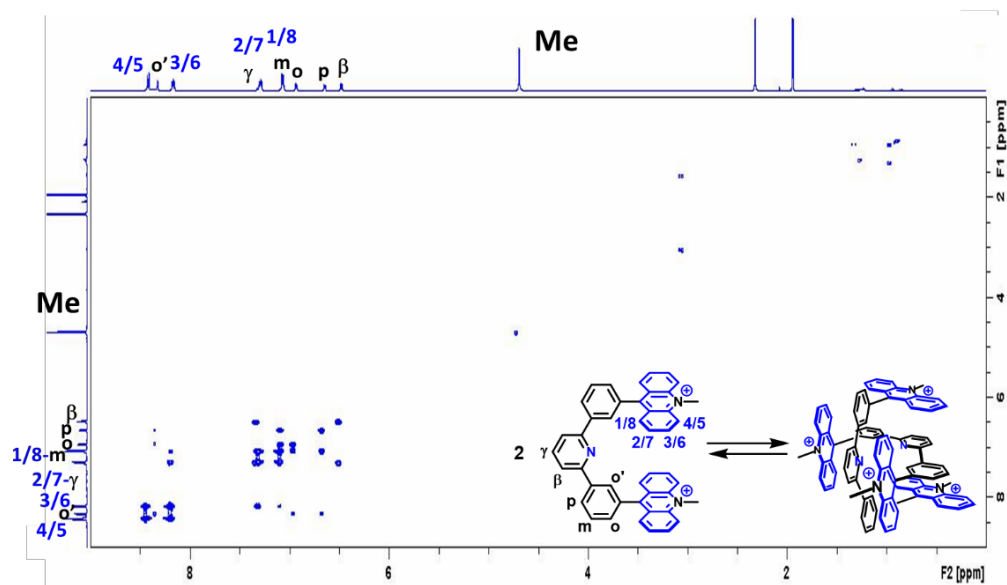


Figure S3.20: ^1H - ^1H COSY 2D-spectrum (600 MHz, CD_3CN , 238 K) spectrum of the dimer of $(\mathbf{1})_2\cdot 4\text{PF}_6$ ($c = 1\cdot 10^{-2} \text{ mol}\cdot\text{L}^{-1}$).

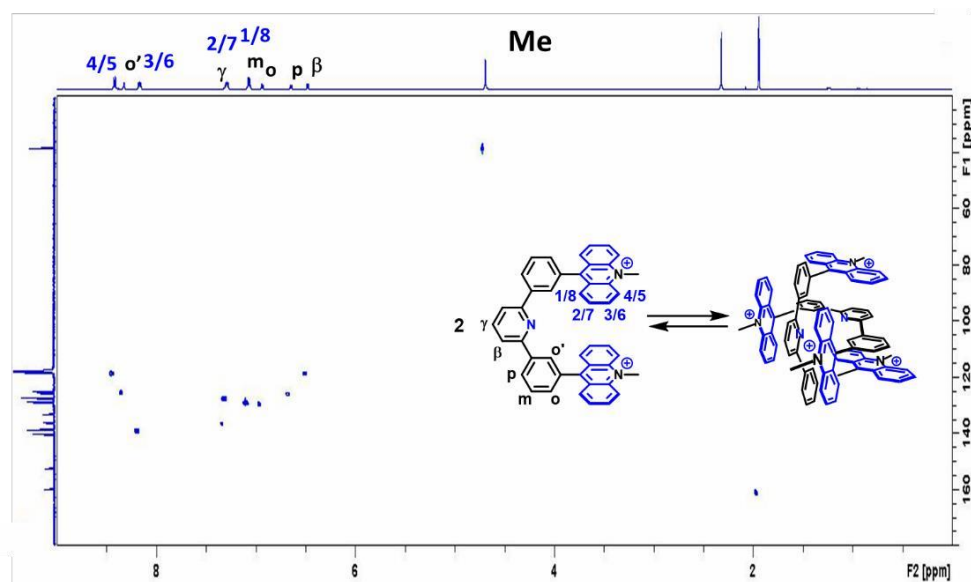


Figure S3.21: ^1H - ^{13}C HSQC 2D-spectrum (600 MHz, CD_3CN , 238 K) spectrum of the dimer of **(1)** $_2\cdot 4\text{PF}_6$ ($c = 1 \cdot 10^{-2} \text{ mol} \cdot \text{L}^{-1}$).

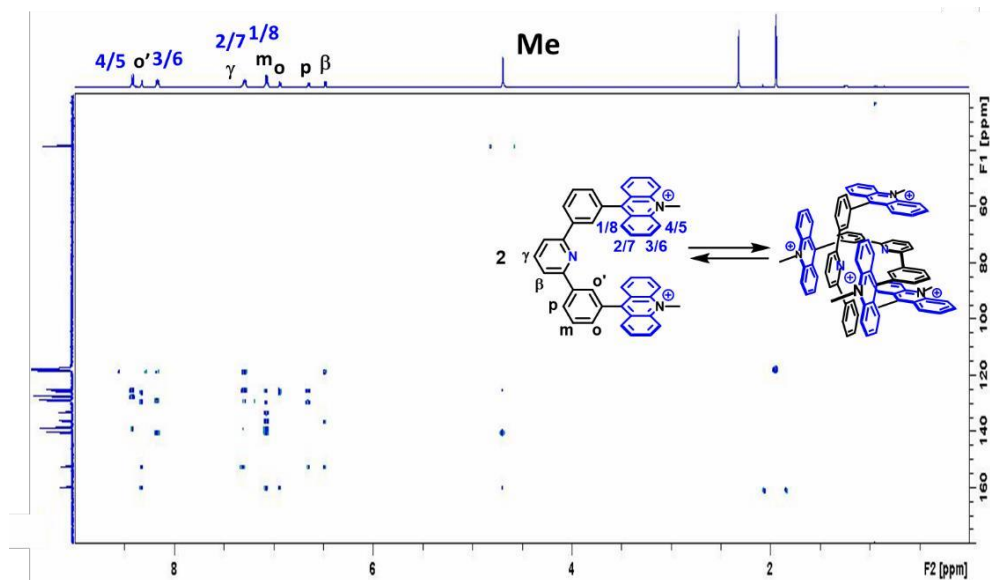


Figure S3.22: ^1H - ^{13}C HMBC 2D-spectrum (600 MHz, CD_3CN , 238 K) spectrum of the dimer of **(1)** $_2\cdot 4\text{PF}_6$ ($c = 1 \cdot 10^{-2} \text{ mol} \cdot \text{L}^{-1}$).

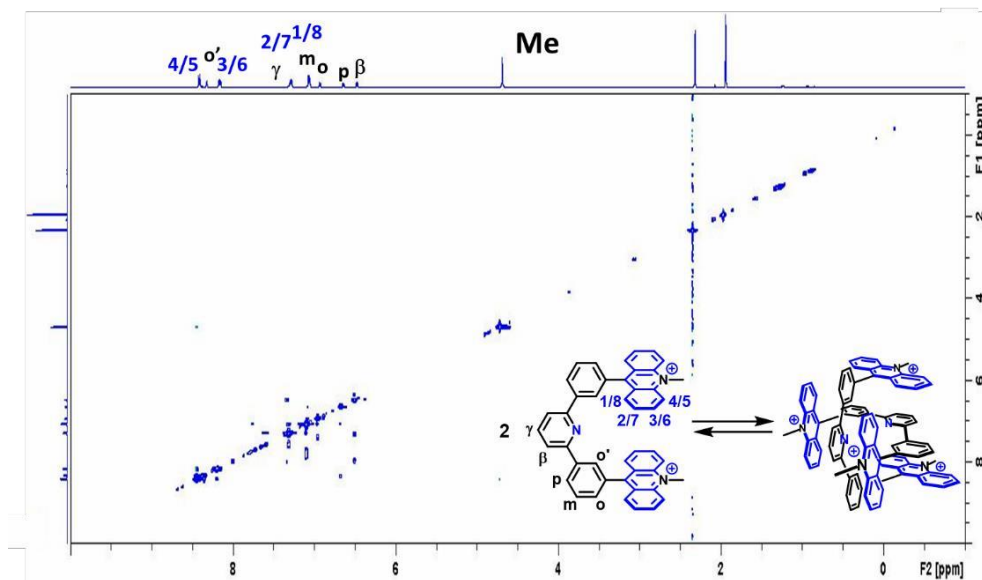


Figure S3.23: ^1H - ^1H NOESY 2D-spectrum (600 MHz, CD_3CN , 238 K) spectrum of the dimer of $(1)_2 \cdot 4\text{PF}_6$ ($c = 1 \cdot 10^{-2} \text{ mol} \cdot \text{L}^{-1}$).

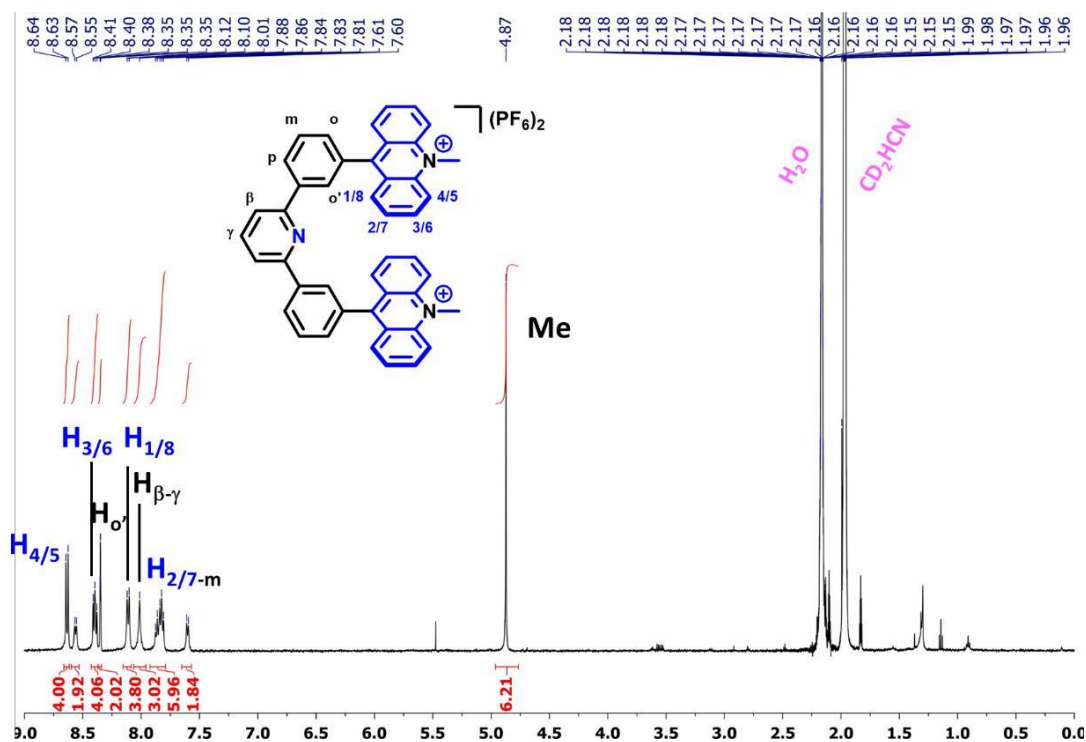


Figure S3.24: ^1H NMR (600 MHz, CD_3CN , 298 K) spectrum of the monomer of $(1)_2 \cdot 4\text{PF}_6$ ($c = 5 \cdot 10^{-4} \text{ mol} \cdot \text{L}^{-1}$).

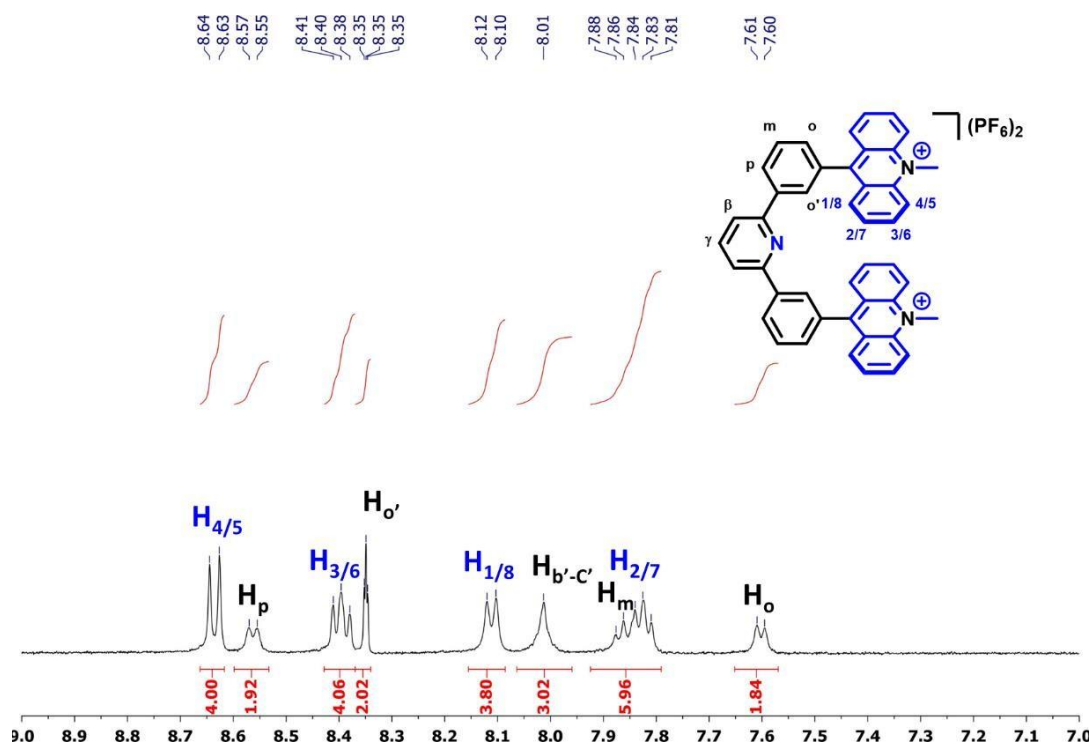


Figure S3.25: ^1H NMR (600 MHz, CD_3CN , 298 K) spectrum of the monomer of **1**·**2PF**₆ ($c = 5 \cdot 10^{-4} \text{ mol} \cdot \text{L}^{-1}$; zoom aromatic region).

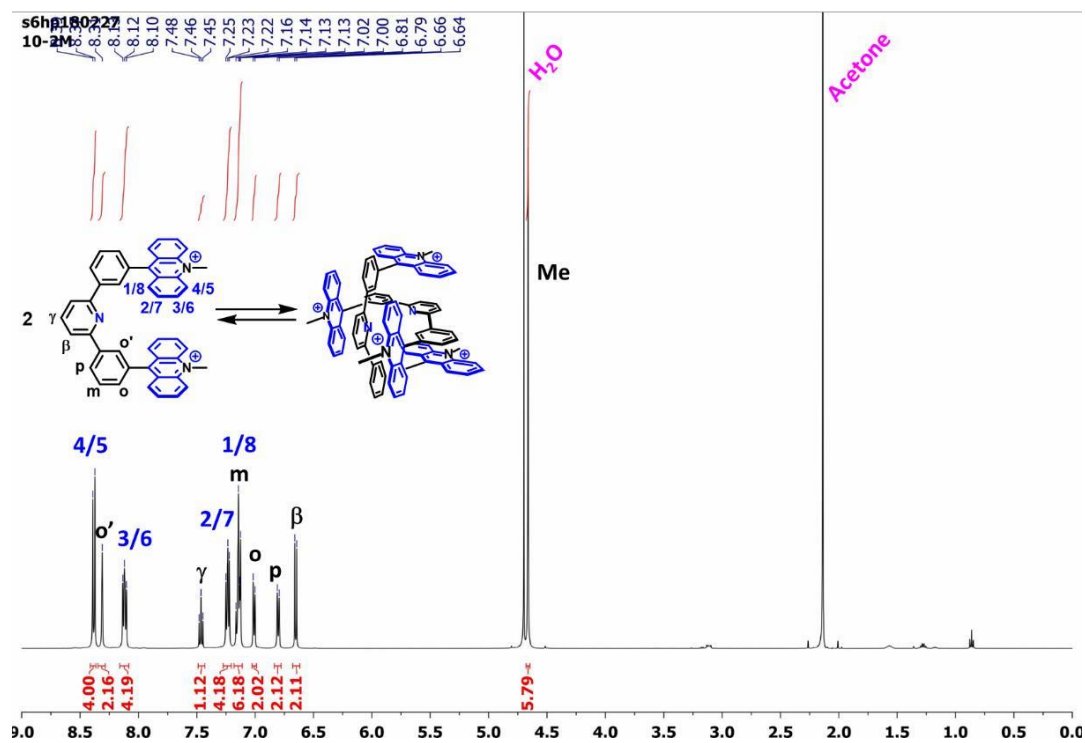


Figure S3.26: ^1H NMR (600 MHz, D_2O , 298 K) spectrum of the dimer of (**1**)₂·**4Cl** ($c = 1 \cdot 10^{-2} \text{ mol} \cdot \text{L}^{-1}$).

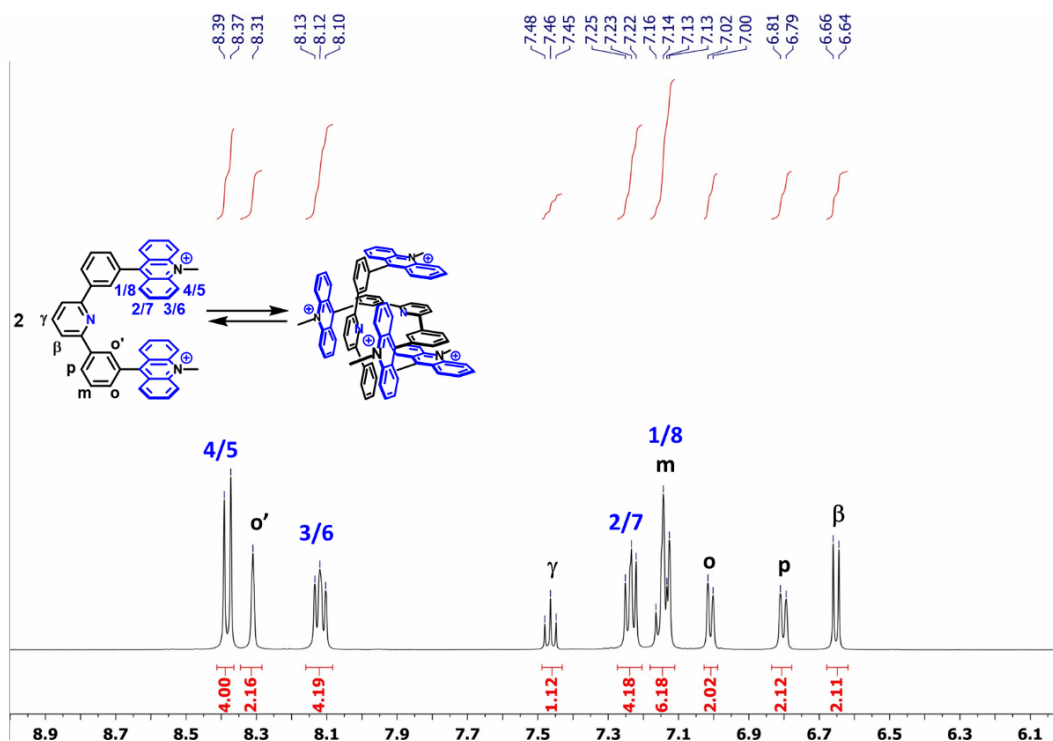


Figure S3.27: ¹H NMR (600 MHz, D₂O, 298 K) spectrum of the dimer of (1)₂·4Cl (*c* = 1·10⁻² mol·L⁻¹; zoom aromatic region).

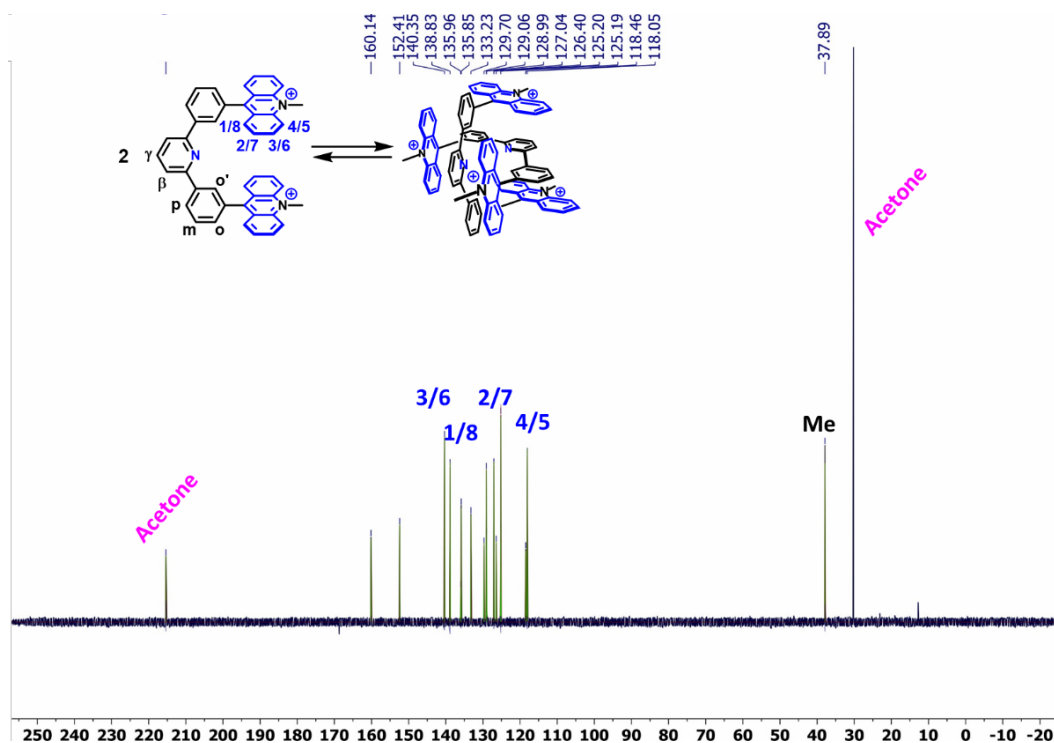


Figure S3.28: ¹³C NMR (150 MHz, D₂O, 298 K) spectrum of the dimer of (1)₂·4Cl (*c* = 1·10⁻² mol·L⁻¹).

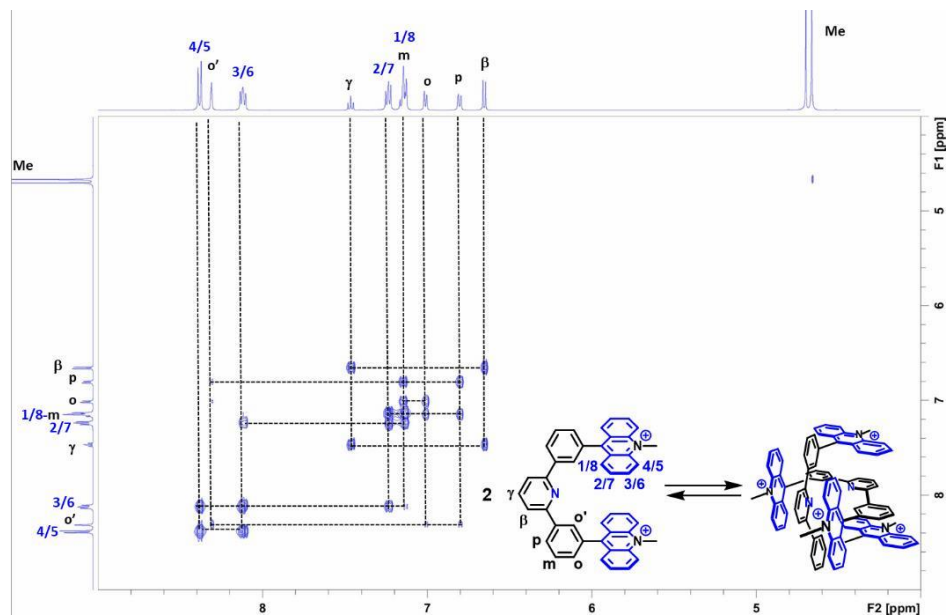


Figure S3.29: ^1H – ^1H COSY 2D-spectrum (600 MHz, D_2O , 298 K) of the dimer of $(\mathbf{1})_2\cdot 4\text{Cl}$ ($c = 1 \cdot 10^{-2} \text{ mol}\cdot\text{L}^{-1}$).

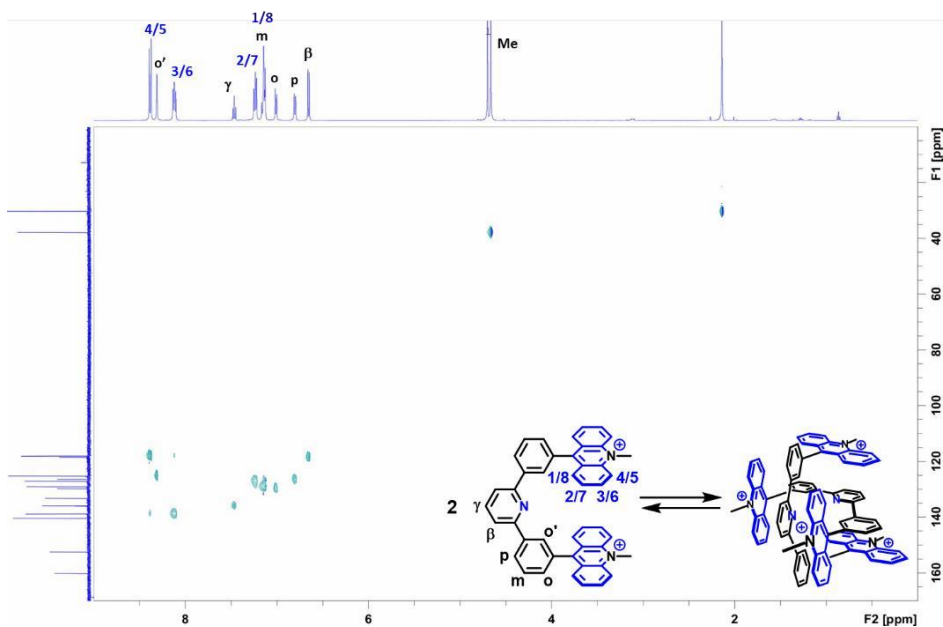


Figure S3.30: ^1H – ^1H HSQC 2D-spectrum (600 MHz, D_2O , 298 K) of the dimer of $(\mathbf{1})_2\cdot 4\text{Cl}$ ($c = 1 \cdot 10^{-2} \text{ mol}\cdot\text{L}^{-1}$).

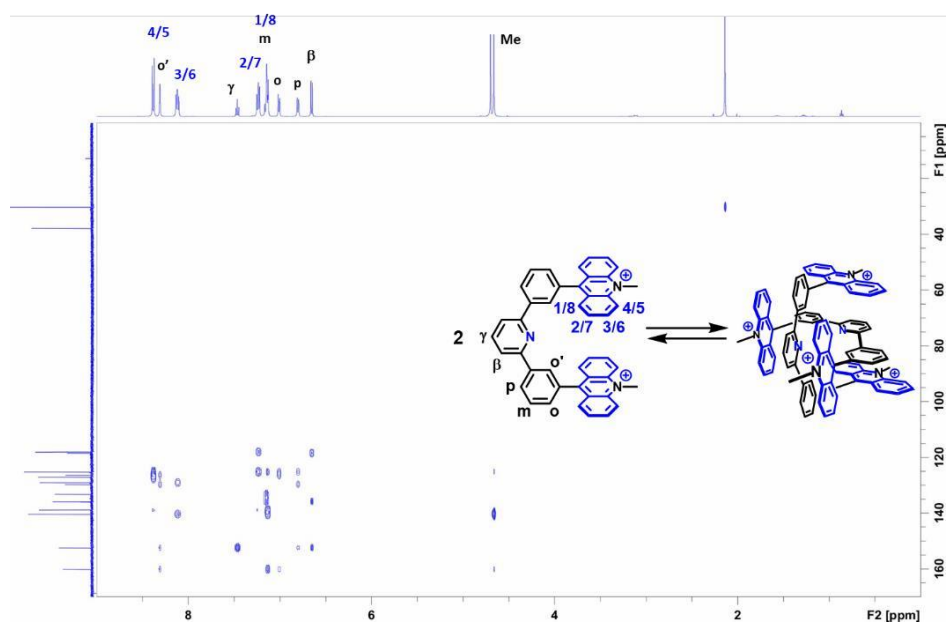


Figure S3.31: ^1H - ^1H HMBC 2D-spectrum (600 MHz, D_2O , 298 K) of the dimer of $(\mathbf{1})_2\cdot\mathbf{4Cl}$ ($c = 1 \cdot 10^{-2} \text{ mol} \cdot \text{L}^{-1}$).

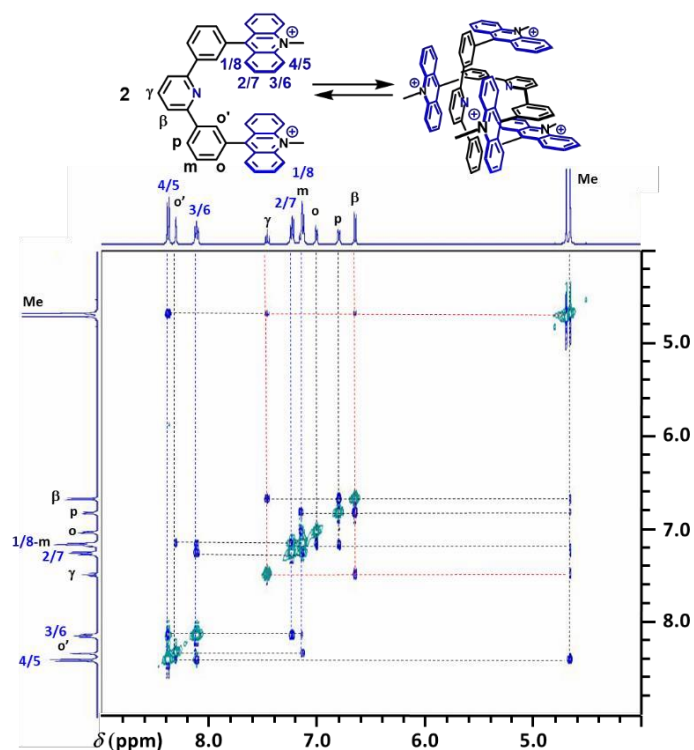
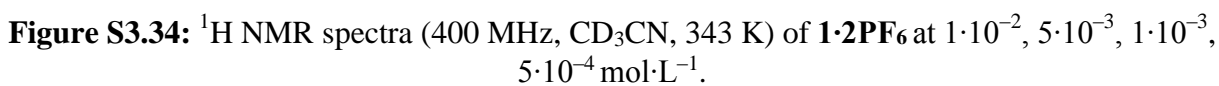


Figure S3.32: ^1H - ^1H NOESY 2D-spectrum (600 MHz, D_2O , 298 K) of the dimer of $(\mathbf{1})_2\cdot\mathbf{4Cl}$ ($c = 1 \cdot 10^{-2} \text{ mol} \cdot \text{L}^{-1}$).



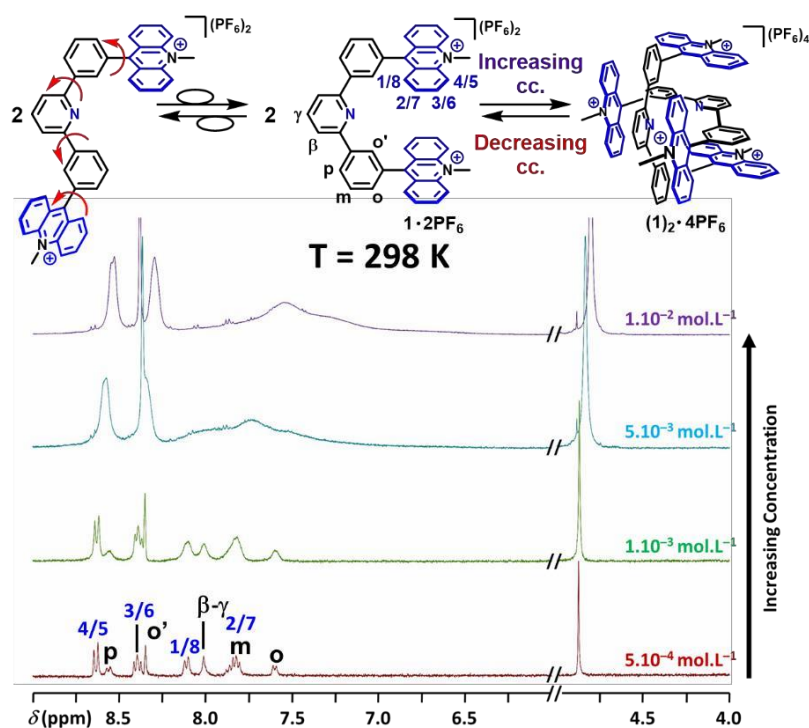


Figure S3.35: ^1H NMR spectra (400 MHz, CD_3CN , 298 K) of $1 \cdot 2\text{PF}_6$ at $1 \cdot 10^{-2}$, $5 \cdot 10^{-3}$, $1 \cdot 10^{-3}$, $5 \cdot 10^{-4} \text{ mol} \cdot \text{L}^{-1}$.

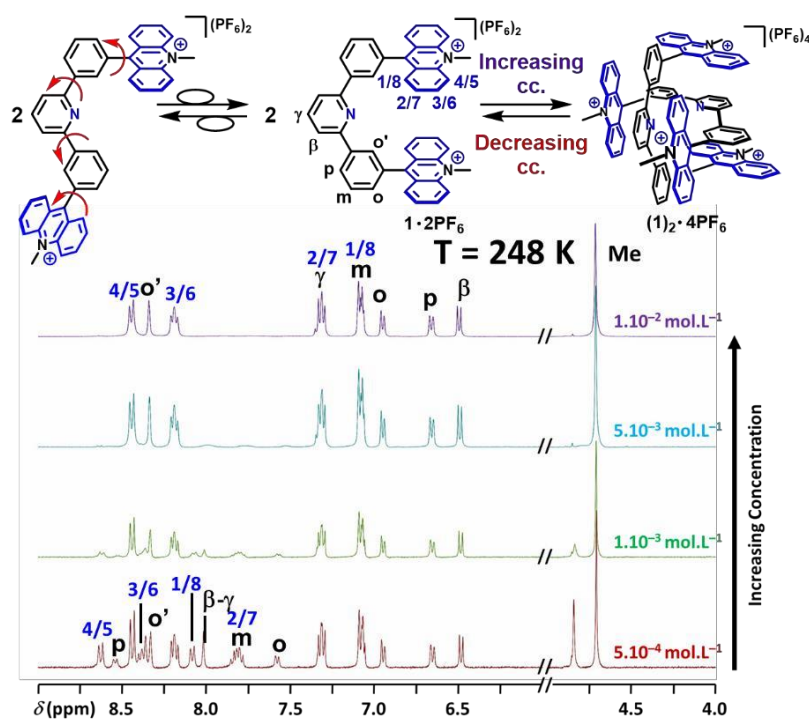


Figure S3.36: ^1H NMR spectra (400 MHz, CD_3CN , 248 K) of $1 \cdot 2\text{PF}_6$ at $1 \cdot 10^{-2}$, $5 \cdot 10^{-3}$, $1 \cdot 10^{-3}$, $5 \cdot 10^{-4} \text{ mol} \cdot \text{L}^{-1}$.

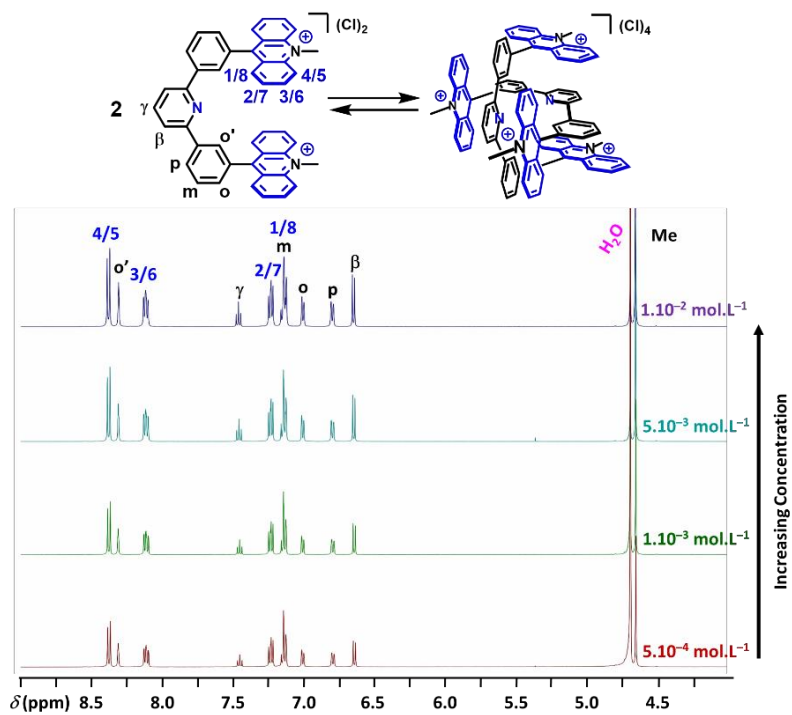


Figure S3.37: ^1H NMR spectra (400 MHz, D_2O , 298 K) of $(\mathbf{1})_2\cdot 4\text{Cl}$ at $1\cdot 10^{-2}$, $5\cdot 10^{-3}$, $1\cdot 10^{-3}$, $5\cdot 10^{-4}\text{ mol}\cdot\text{L}^{-1}$.

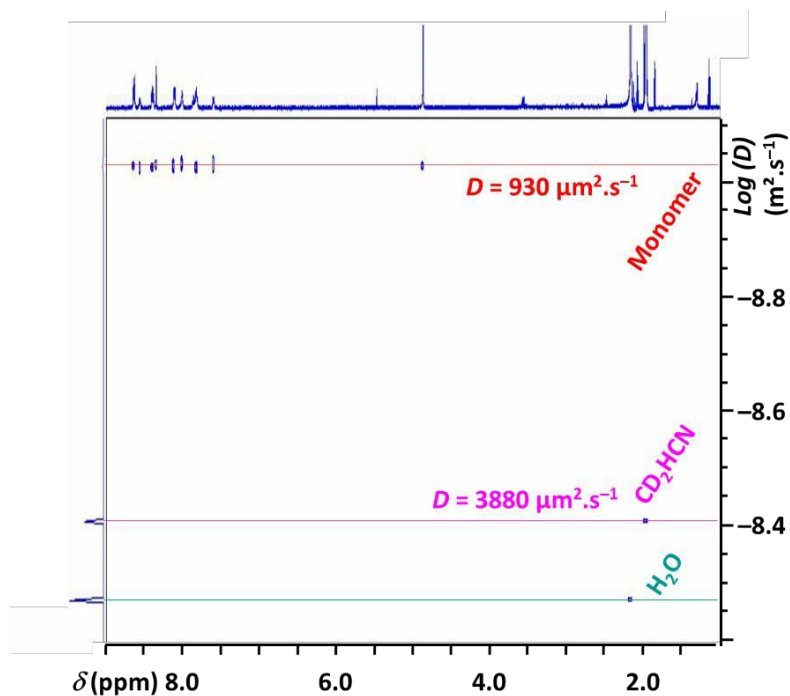


Figure S3.38: ^1H DOSY spectrum (600 MHz, CD_3CN , 298 K) spectrum of $\mathbf{1}\cdot 2\text{PF}_6$ at $5\cdot 10^{-4}\text{ mol}\cdot\text{L}^{-1}$.

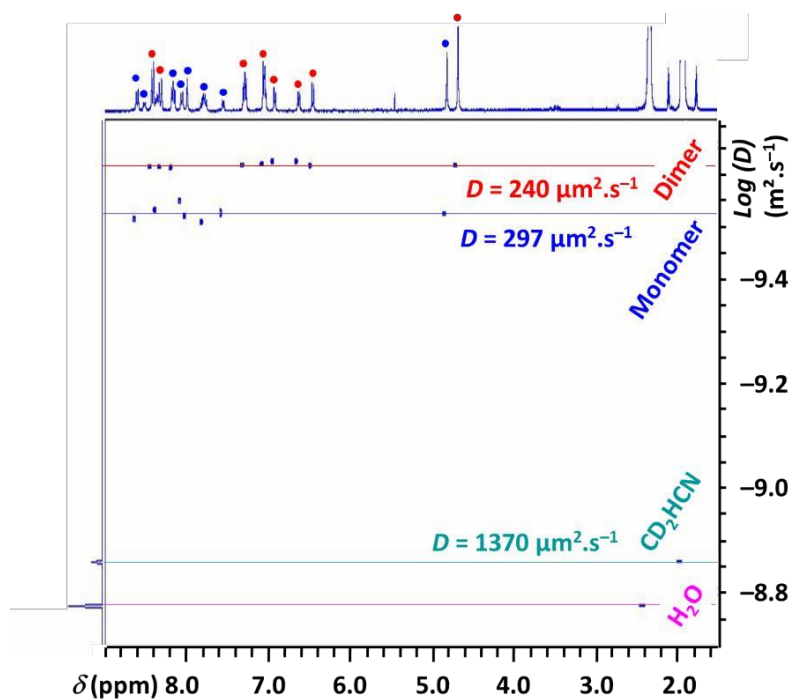


Figure S3.39: ^1H DOSY spectrum (600 MHz, CD_3CN , 238 K) spectrum of $1\cdot 2\text{PF}_6$ at $5\cdot 10^{-4} \text{ mol}\cdot\text{L}^{-1}$.

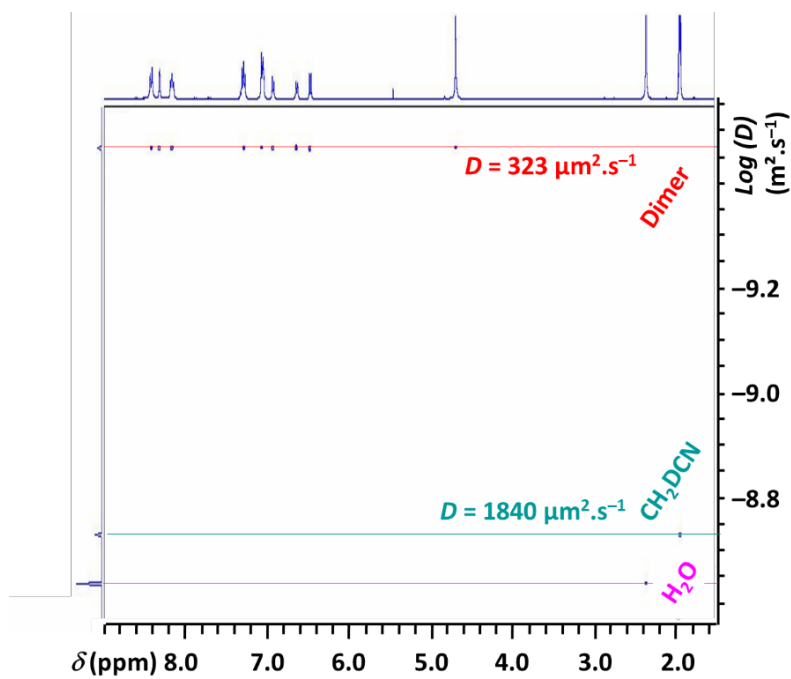


Figure S3.40: ^1H DOSY spectrum (600 MHz, CD_3CN , 238 K) spectrum of $1\cdot 2\text{PF}_6$ at $1\cdot 10^{-2} \text{ mol}\cdot\text{L}^{-1}$.

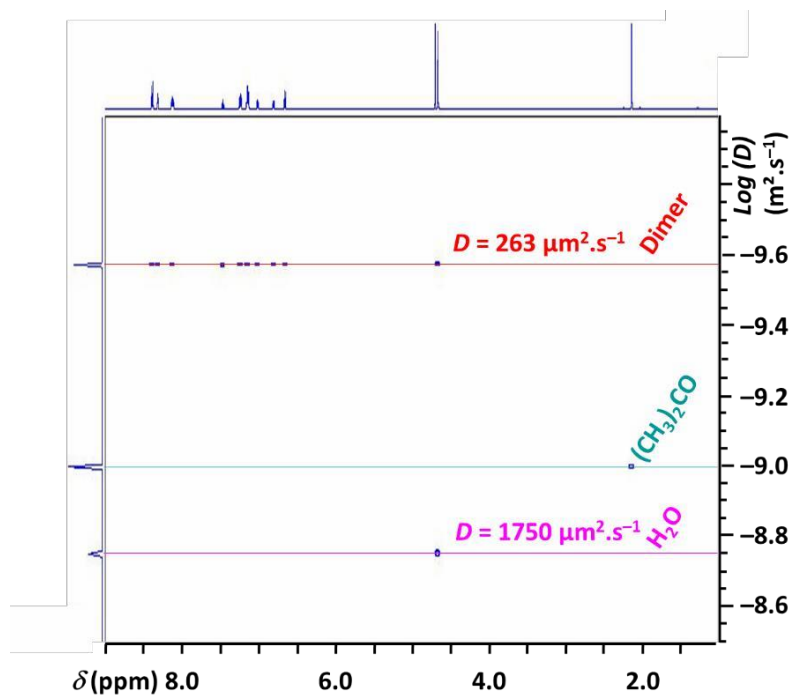


Figure S3.41: ^1H DOSY spectrum (600 MHz, D_2O , 298 K) spectrum of $(\mathbf{1})_2\cdot 4\text{Cl}$ at $1\cdot 10^{-2}\text{ mol}\cdot\text{L}^{-1}$.

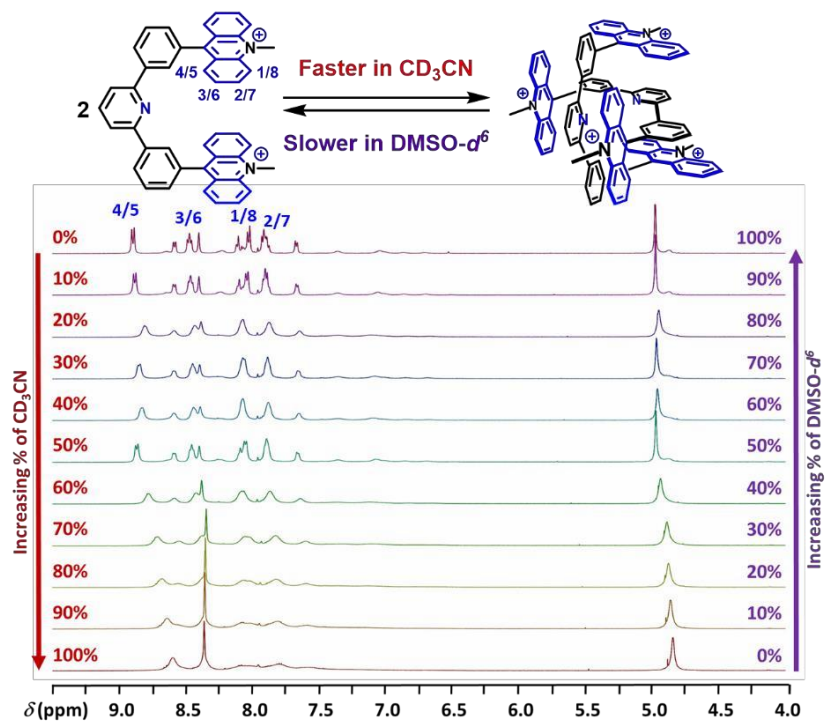


Figure S3.42: ^1H NMR (500 MHz, 298 K, $c = 3\cdot 10^{-3}\text{ mol}\cdot\text{L}^{-1}$) spectra of $\mathbf{1.2PF}_6$ from pure CD_3CN to pure $\text{DMSO}-d^6$.

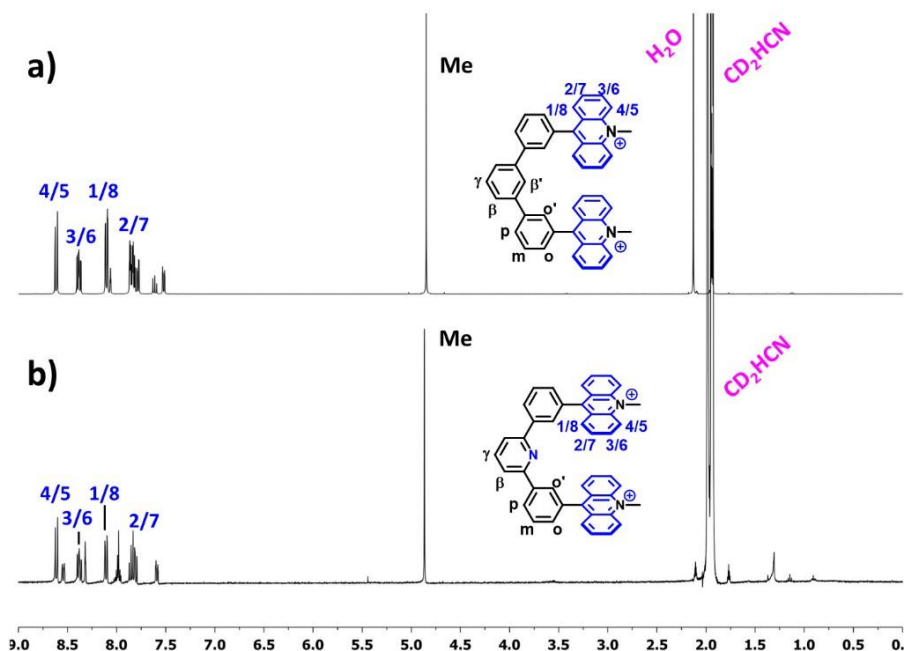


Figure S3.43: ^1H NMR (400 MHz, CD_3CN , 298 K) spectra of a) the triphenyl-*bis*-acridinium receptor^[S1] and b) $1 \cdot 2\text{PF}_6$ ($c = 5 \cdot 10^{-4} \text{ mol} \cdot \text{L}^{-1}$).

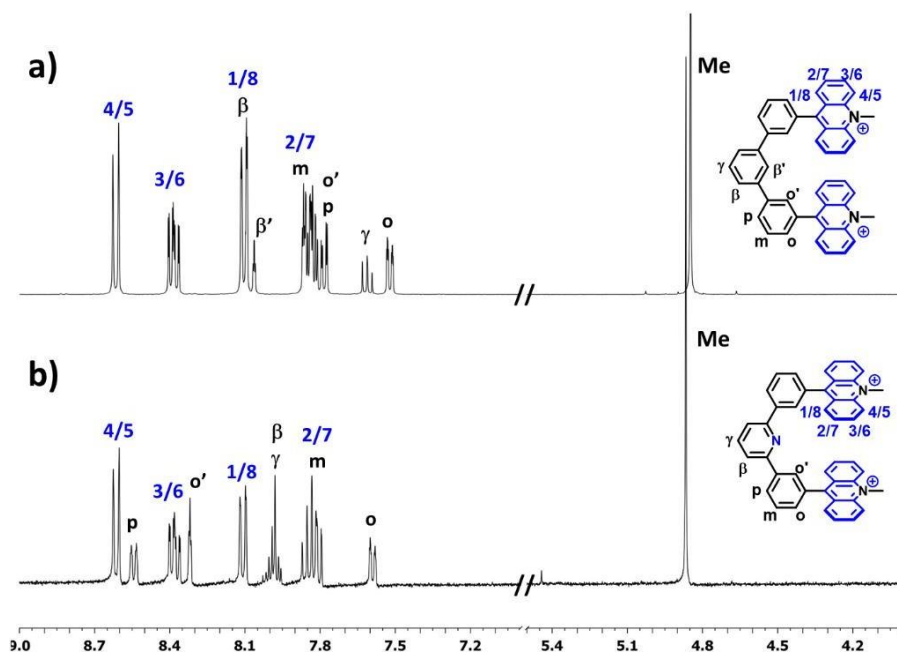


Figure S3.44: ^1H NMR (400 MHz, CD_3CN , 298 K) spectra of a) the triphenyl-*bis*-acridinium receptor^[S1] and b) $1 \cdot 2\text{PF}_6$ ($c = 5 \cdot 10^{-4} \text{ mol} \cdot \text{L}^{-1}$; zoom of the aromatic region).

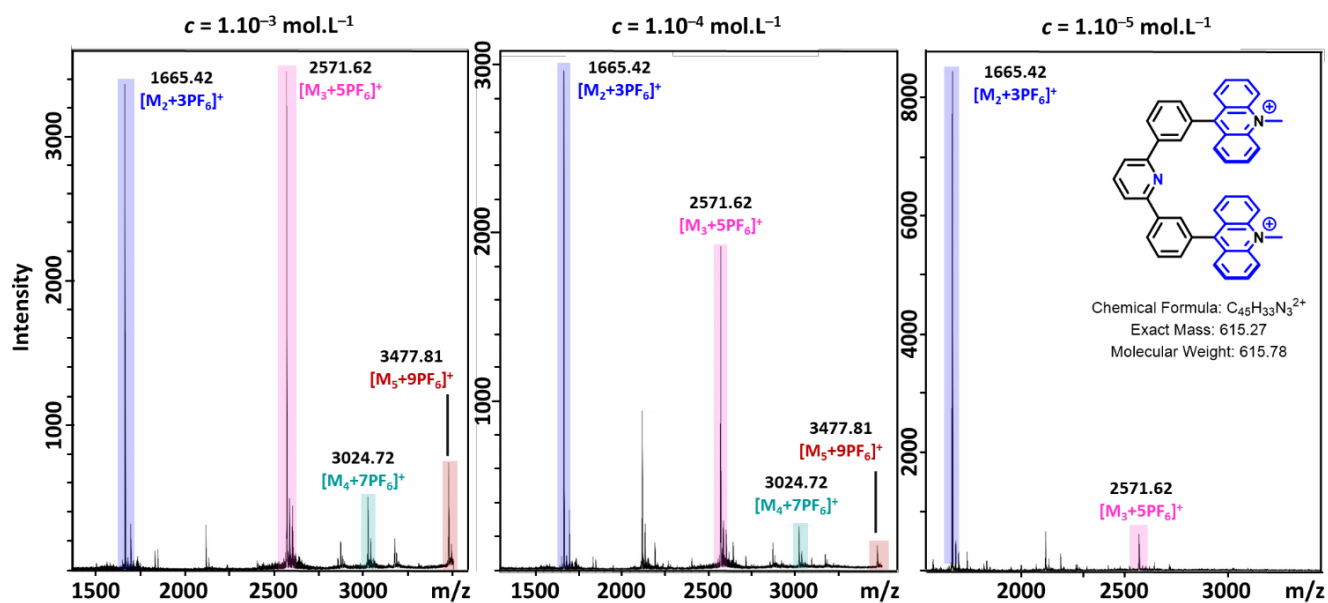


Figure S3.45: Mass Spectra (ESI-TOF) of a solution of $1 \cdot 2\text{PF}_6$ in CH_3CN injected at different concentrations: $1 \cdot 10^{-3}$, $1 \cdot 10^{-4}$, $1 \cdot 10^{-5} \text{ mol}\cdot\text{L}^{-1}$ (zoom on the aggregate region).

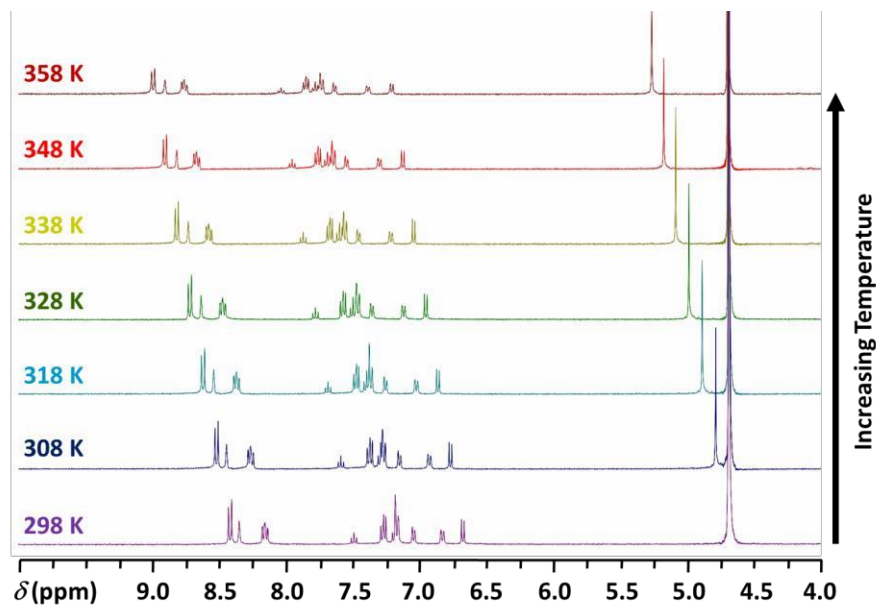


Figure S3.46: ^1H NMR (600 MHz, D_2O) spectra of $(1)_2 \cdot 4\text{Cl}$ recorded from 298 K to 358 K.

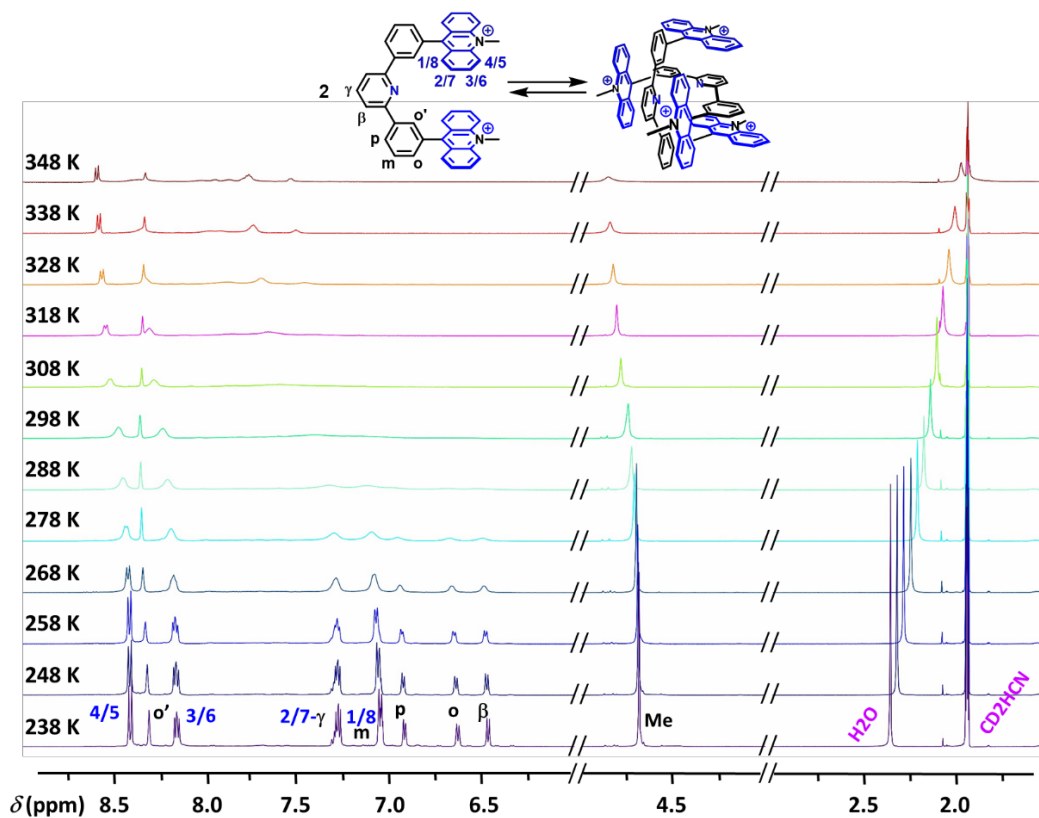


Figure S3.47: ^1H NMR (600 MHz, CD_3CN) spectra of $1\cdot 2\text{Cl}$ recorded from 238 K to 348 K ($c = 1\cdot 10^{-2} \text{ mol}\cdot\text{L}^{-1}$).

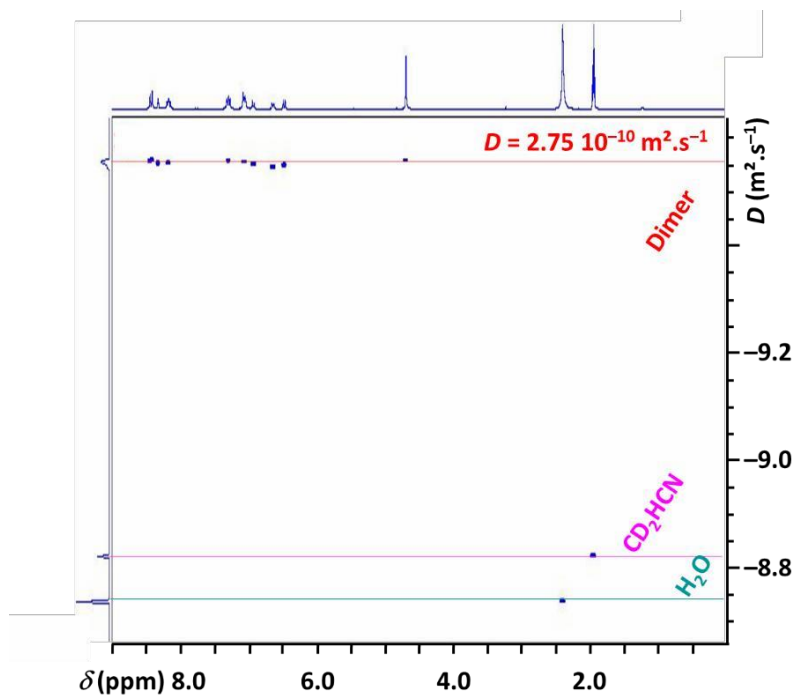


Figure S3.48: ^1H DOSY spectrum (300 MHz, CD_3CN , 238 K) spectrum of $(1)_2\cdot 4\text{PF}_6$ at $1\cdot 10^{-2} \text{ mol}\cdot\text{L}^{-1}$.

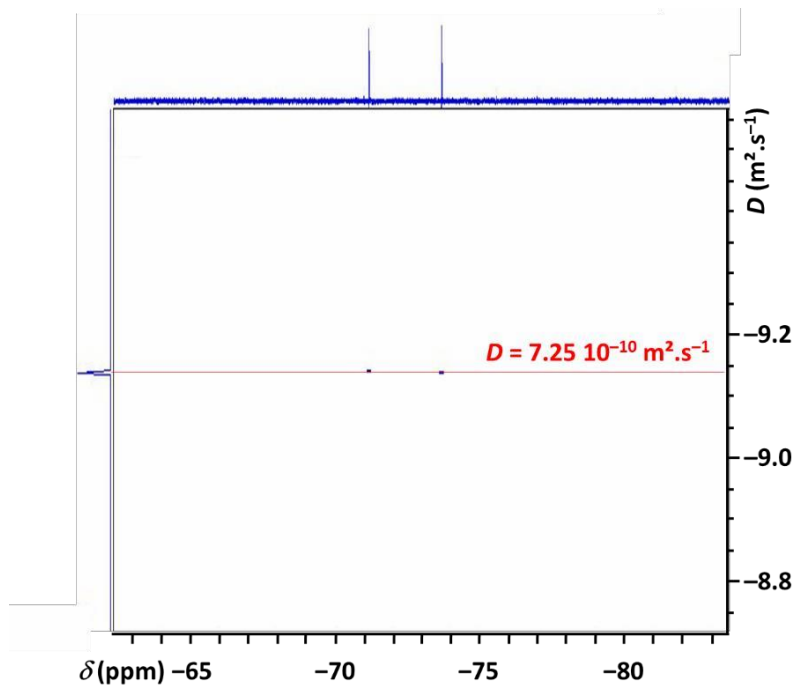


Figure S3.49: ^{19}F DOSY spectrum (300 MHz, CD_3CN , 238 K) spectrum of $(\mathbf{1})_2 \cdot 4\text{PF}_6$ at $1 \cdot 10^{-2} \text{ mol} \cdot \text{L}^{-1}$.

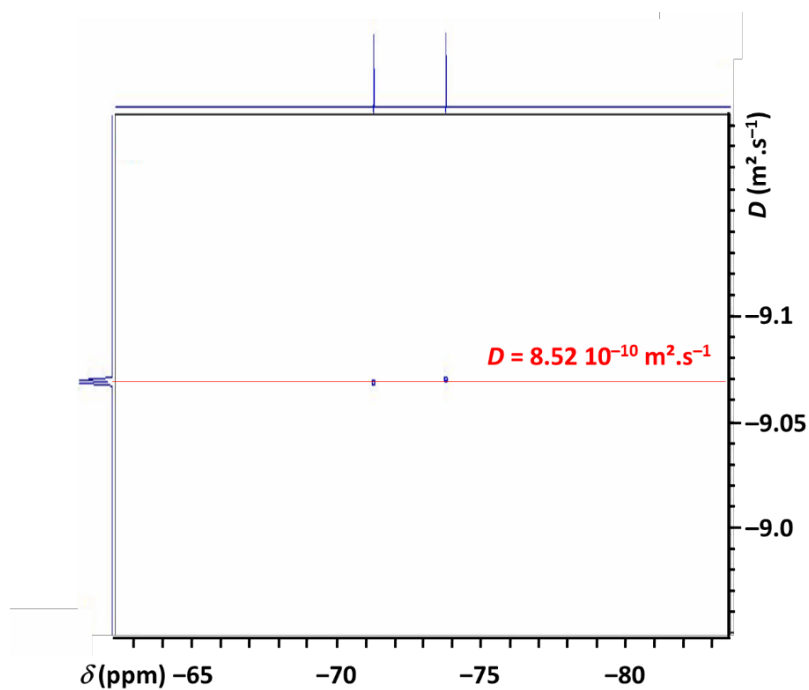


Figure S3.50: ^{19}F DOSY spectrum (300 MHz, CD_3CN , 238 K) spectrum of KPF_6 at $1 \cdot 10^{-2} \text{ mol} \cdot \text{L}^{-1}$.

4. UV-Vis Characterizations of **1.2PF₆**

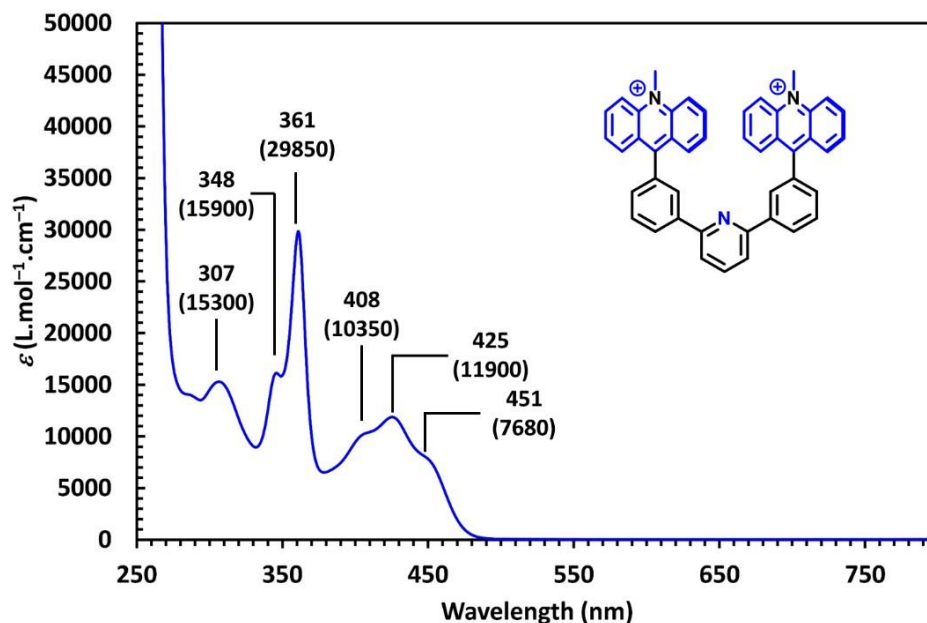


Figure S4.1: UV-Vis spectrum (CH_3CN , $l = 0.1$ cm, 298 K) of **1.2PF₆** (blue, $c = 5 \cdot 10^{-4}$ mol·L⁻¹).

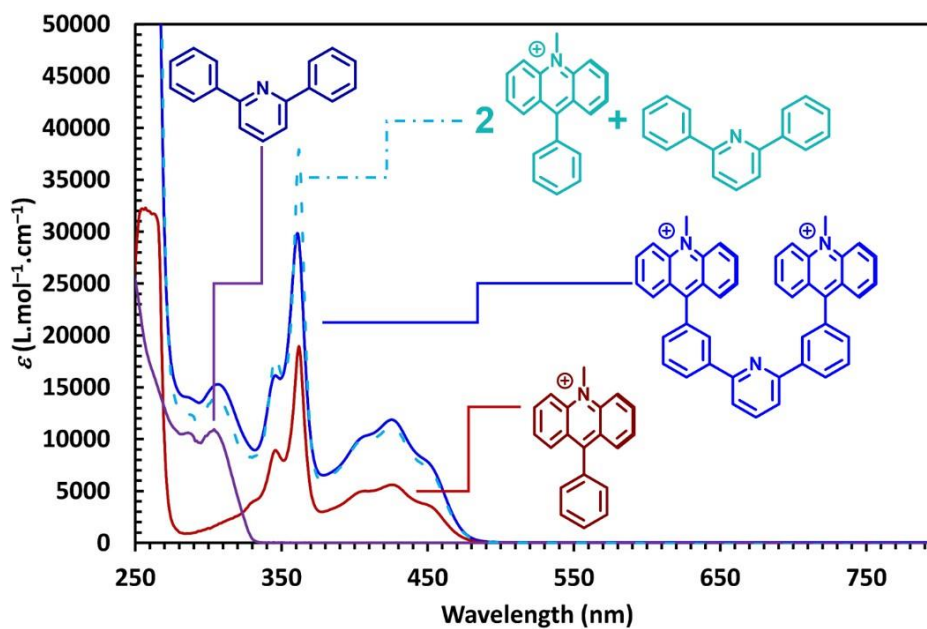


Figure S4.2: UV-Vis spectra (CH_3CN , $l = 0.1$ cm, 298 K) of **1.2PF₆** (blue, $c = 5 \cdot 10^{-4}$ mol·L⁻¹), 2,6-diphenylpyridine (purple, $c = 5 \cdot 10^{-4}$ mol·L⁻¹), 9-phenyl-*N*-acridinium (red, $c = 5 \cdot 10^{-4}$ mol·L⁻¹) and the sum of 2,6-diphenylpyridine and twice of 9-phenyl-*N*-acridinium (light blue).

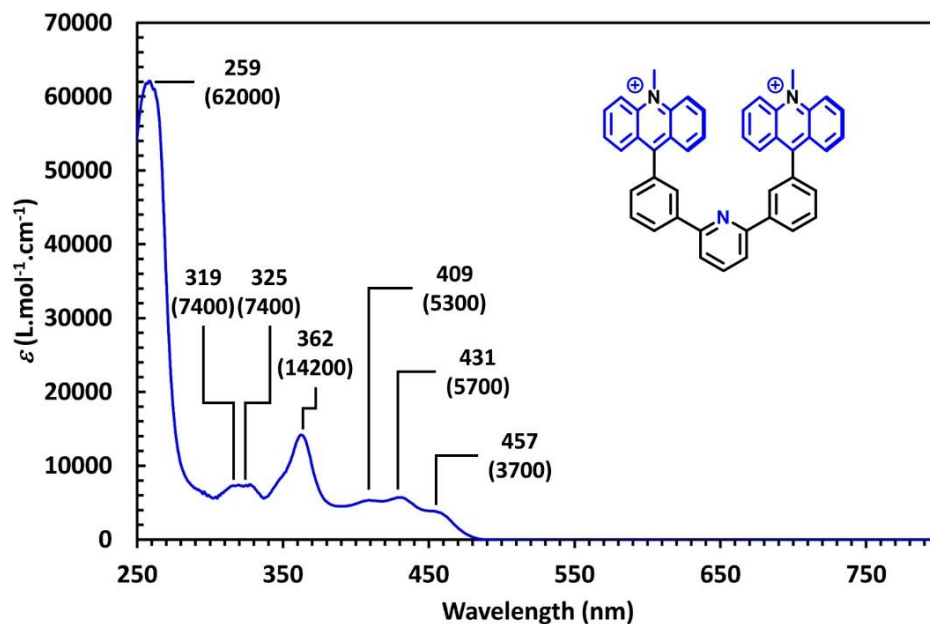


Figure S4.3: UV-Vis spectrum (H_2O , $l = 0.1 \text{ cm}$, 298 K) of $(\mathbf{1})_2 \cdot 4\text{Cl}$ (blue, $c = 5 \cdot 10^{-4} \text{ mol} \cdot \text{L}^{-1}$).

5. Crystallographic Data of $(\mathbf{1})_2 \cdot 4\text{PF}_6$

Within the crystal lattice, the dimers are orientated in a head-to-tail manner along the median of the b and c axis. Dimers of $\mathbf{1} \cdot 2\text{PF}_6$ are arranged according to a herringbone structure along the b and c axis and are organized in a ladder type manner along the a axis.

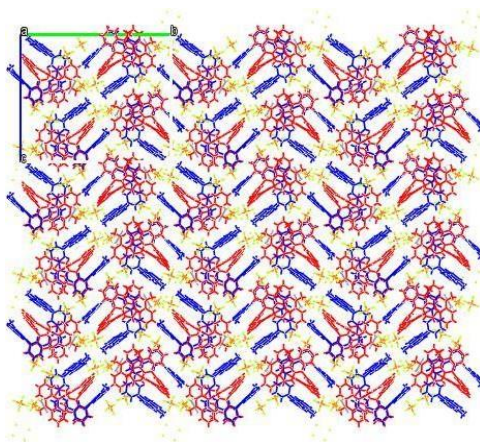


Figure S5.1: Representation of the crystal packing along the a axis.

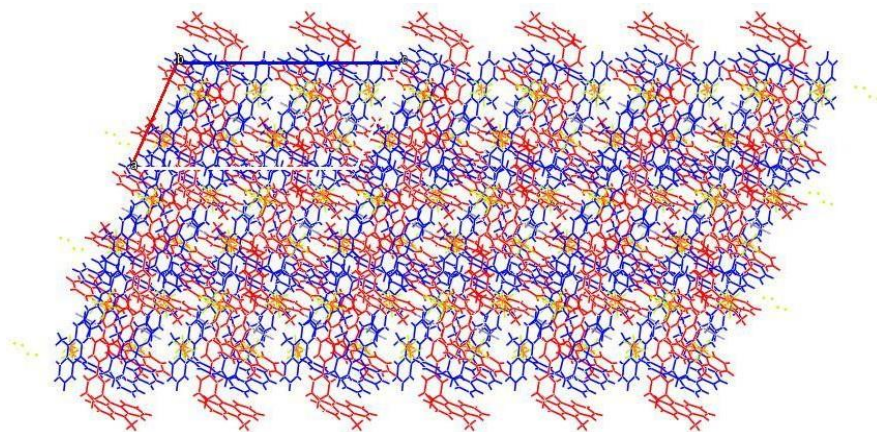


Figure S5.2: Representation of the crystal packing along the *b* axis.

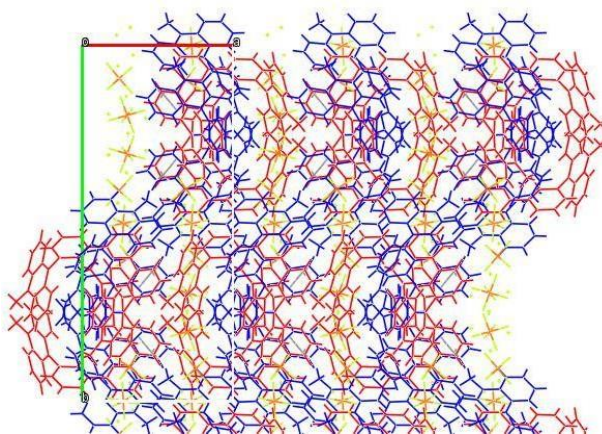


Figure S5.3: Representation of the crystal packing along the *c* axis.

6. References

- [S1] A. Gosset, Z. Xu, F. Maurel, L.-M. Chamoreau, S. Nowak, G. Vives, C. Perruchot, V. Heitz and H.-P. Jacquot de Rouville, *New J. Chem.*, **2018**, 42, 4728–4734.
- [S2] G. R. Fulmer, A. J. M. Miller, N. H. Sherden, H. E. Gottlieb, A. Nudelman, B. M. Stoltz, J. E. Bercaw, and K. I. Goldberg, *Organometallics*, **2010**, 29, 2176–2179
- [S3] Y. Cohen, L. Avram and L. Frish, *Angew. Chem. Int. Ed.*, **2005**, 44, 520–554.
- [S4] M. Holz, X. Mao, D. Seiferling and A. Sacco, *J. Chem. Phys.*, **1996**, 104, 669–679.
- [S5] “M86-E01078 APEX2 User Manual”, Bruker AXS Inc., Madison, USA, **2006**.
- [S6] G. M. Sheldrick, *Acta Crystallogr.* **2015**, A71, 3–8.
- [S7] G. M. Sheldrick, *Acta Crystallogr.* **2008**, A64, 112–122.